

# Isotopic effects in spallation and fission reactions and mass-spectrometer investigation of them with 1-GeV protons

B. N. Belyaev, V. D. Domkin, and V. S. Mukhin  
V. G. Khlopin Radium Institute, St. Petersburg

Fiz. Elem. Chastits At. Yadra **23**, 993–1034 (July–August 1992)

An “in line” mass spectrometer has been used to investigate the isotope dependences of the yields of the product nuclei in nuclear reactions induced by 1-GeV protons on targets of light nuclei,  $^{12}\text{C}(p,X)^{6-9}\text{Li}$ ,  $^{13}\text{C}(p,X)^{6-9}\text{Li}$ , medium nuclei,  $^{90}\text{Zr}(p,X)^{74-86}\text{Rb}$ ,  $^{91}\text{Zr}(p,X)^{76-88}\text{Rb}$ ,  $^{71-84}\text{Br}$ ,  $^{94}\text{Zr}(p,X)^{76-90}\text{Rb}$ , heavy nuclei,  $^{176-192}\text{Rb}$ ,  $^{80-94}\text{Sr}$ ,  $^{118-133}\text{Cs}$ ,  $^{42-48}\text{K}$ ,  $^{79-97}\text{Rb}$ ,  $^{121-146}\text{Cs}$ , and also  $^{81-94}\text{Rb}$  at  $E_p=0.75$  GeV. The high-precision measurements of the relative yields of some product isotopes have been used in a systematic study of even–odd and shell effects in nuclear reactions induced by intermediate-energy protons. Existing reaction models have been used to calculate the yields of the product nuclei for a series of isotope targets. Aspects of the spallation and fission reaction mechanisms for reactions induced by intermediate-energy protons are discussed on the basis of an analysis and comparison of the calculated and experimental isotope distributions.

## ISOTOPE DISTRIBUTIONS OF THE PRODUCT NUCLEI FROM SPALLATION OF LIGHT AND MEDIUM NUCLEI. ISOTOPIC EFFECTS

In mass-spectrometer measurements “in line” with an accelerator, the intervals of time between the formation of the products of the nuclear reactions and the measurement of the mass spectra are short compared with the half-lives of the majority of the produced nuclides. Therefore, the corrections for their decay and accumulation are small and are readily taken into account in the analysis of the measurements. This fact, and also the high accuracy with which the mass-spectrum line intensities are measured guarantee the important advantages of this method in the investigation of the fine structure in the isotope distributions of the products of nuclear reactions in the range of half-lives  $0.1 \text{ sec} \leq T_{1/2} \leq \infty$  of the products. In investigations of the product yields by the radiochemical method, such a large range of nuclides is not accessible. However, to determine the magnitude of the production cross sections of the product nuclei the mass-spectrometric data must be normalized by the absolute independent yields of one or several nuclides determined by  $\alpha$ ,  $\beta$ , or  $\gamma$  spectrometry in conjunction with the radiochemical methods.

In this section, we present the results of an investigation of the influence of nuclear structure on the spallation reaction cross sections of some light and medium nuclei induced by protons with energy  $E_p=1$  GeV. The investigation was based on measurements of the relative independent yields of Li, Br, and Rb isotopes by means of a mass spectrometer “in line” with the synchrocyclotron of the B. P. Konstantinov St. Petersburg Institute of Nuclear Physics.<sup>1</sup>

The experimental yields of the isotopes of the product nuclei with even numbers of neutrons are systematically above, and those with odd numbers of neutrons below, the parabolic curve of the type (1) that approximates them by an amount  $\Delta$  which is approximately equal to half the

difference between the yields of the odd and even isotopes:

$$\ln Y_A \sim C_0 + C_1 A + C_2 A^2, \quad (1)$$

$$Y_A \cong Y_A^{(0)} [1 + (-1)^{A-Z} \Delta], \quad (2)$$

where  $Y_A$  is the experimental yield of the nuclide with mass number  $A$  and proton number  $Z$ , and  $Y_A^{(0)}$  is the yield of this nuclide determined from the approximating curve.

The simplest way of obtaining a numerical estimate of the even–odd isotopic effect  $\Delta$  in the isotope distributions of nuclear-reaction products was proposed in Ref. 2, in which it was shown that  $\Delta$  can be expressed in terms of the third difference of the logarithms of the yields of four neighboring isotopes:

$$\Delta = \frac{(-1)^{A-Z}}{8} \ln \left[ \frac{Y_A}{Y_{A+3}} \left( \frac{Y_{A+2}}{Y_{A+1}} \right)^3 \right]. \quad (3)$$

This expression holds more accurately, the nearer the real values of  $Y_A$  are to the approximating curve and the smaller is the difference between the values of  $\Delta$  for different sections of the isotope distributions. If the deviations of the yields from the approximating curve of the type (1) differ in absolute magnitude, then in such a case the expression (1) gives a certain averaged value of the even–odd effects.

## Role of nuclear structure in the light-nucleus $^{12,13}\text{C}(p,X)^{6-9}\text{Li}$ spallation reactions

When high-energy protons interact with nuclei, the influence of the nuclear structure is manifested to the greatest extent in the spallation of light nuclei.<sup>3,4</sup>

Among the characteristic features of such reactions, one must include the very strong impact on the target nuclei, as a consequence of which it is difficult to establish whether a particular product is a residual nucleus or a cluster knocked out in the fast stage of the reaction. In the first of these cases, one will suppose that the magnitude of the even–odd effect is determined by the individual prop-

TABLE I. Relative independent yields of lithium isotopes resulting from spallation of  $^{12}\text{C}$  and  $^{13}\text{C}$  nuclei induced by 1-GeV protons (the data are normalized to the  $^6\text{Li}$  yield).

Product Target	$^6\text{Li}$	$^7\text{Li}$	$^8\text{Li}$	$^9\text{Li}$
$^{12}\text{C}$	1	$0.93 \pm 0.04$	$0.042 \pm 0.009$	$0.007 \pm 0.002$
$^{13}\text{C}$	1	$1.58 \pm 0.06$	$0.16 \pm 0.01$	$0.032 \pm 0.004$

erties of the product nuclei themselves, whereas in the second case an influence of the structure of the original nuclei must also be manifested. For the investigation of the mechanism of spallation reactions of light nuclei and of the role of nuclear structure in these reactions, data on the independent yields of the product nuclei for targets with different isotopic composition are of definite interest.

To obtain such data, we measured the relative yields of the four lithium isotopes  $^6\text{--}^9\text{Li}$  resulting from the interaction of 1-GeV protons with  $^{12}\text{C}$  nuclei (enrichment 98.9%) and  $^{13}\text{C}$  nuclei (enrichment 91%). The results of the measurements, normalized to the  $^6\text{Li}$  yield, are presented in Table I and shown by the points in Fig. 1.

The errors in the measurements given here take into account the errors in the determination of the time of extraction of the lithium from the target and the monitoring of the proton beam by the ionization chamber, and also the statistical uncertainty in the line intensities of the lithium mass spectrum. These data include corrections for the decay of  $^8,9\text{Li}$  and  $^6,8\text{He}$ , for the yield of lithium from the rhenium casing of the target, for the incomplete enrichment of the  $^{13}\text{C}$  target (91%), and for the ion mass-discrimination effect in the multiplier.

In Fig. 1, the continuous curves are the results of approximation of the experimental data by a quasi-Gaussian distribution with respect to  $A$ , which is the basis of several semiempirical formulas.<sup>3,5</sup> The actual yields of Li isotopes with even and odd numbers of neutrons lie above and below these curves, respectively. The even-odd isotopic effect

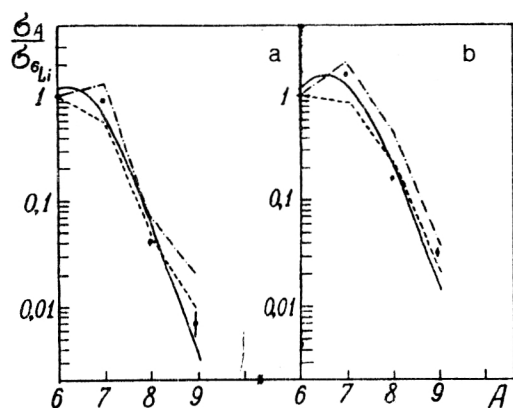


FIG. 1. Relative yields of  $^6\text{--}^9\text{Li}$  isotopes resulting from spallation of  $^{12}\text{C}$  (a) and  $^{13}\text{C}$  (b) induced by protons with  $E_p=1$  GeV. The lines and curves join yields calculated in accordance with formulas taken from the following studies: Ref. 5 (continuous curve), Ref. 6 (dashed line), and Ref. 7 (chain line).

is reproduced somewhat better by the broken lines, which show the results of the calculations of the relative yields of the considered product nuclei in accordance with formulas proposed by different authors for the process of fragmentation of nuclei.<sup>6,7</sup> These formulas take into account the energy of separation of the fragments from the target nuclei, the value of which is influenced by the structure of these nuclei. Table II gives the experimental values of the even-odd effect that we obtained in the  $^{12}\text{C}$  and  $^{13}\text{C}$  spallation reactions and the magnitude of this effect predicted in the framework of some phenomenological models of fragmentation.

The calculated values of the effect agree satisfactorily with the experimental values for the  $^{12}\text{C}$  target and deviate strongly for the spallation of  $^{13}\text{C}$  nuclei, which have an asymmetric nucleon composition.

A possible explanation of this could be the fact that the calculations did not take into account the change in the structure of the residual nuclei and, accordingly, the fragment separation energies as a result of the emission of cascade particles. In reality, it is not the target nuclei that decay, as was assumed in the models, but the remnant formed after the fast stage of the reaction.

#### Zr( $p,4pxn$ )Rb and Zr( $p,6pxn$ )Br reactions

We studied the influence of the isotopic composition of the targets and residual product nuclei on their yields in the Zr( $p,4pxn$ )Rb and Zr( $p,6pxn$ )Br spallation reactions induced by 1-GeV protons. The targets were zirconium isotopes:  $^{90}\text{Zr}$  (enrichment 96.8%),  $^{91}\text{Zr}$  (81.3%), and  $^{94}\text{Zr}$  (91.2%). The method made it possible to determine the relative yields of the Rb and Br isotopes over a wide interval of masses (13–15) and with an accuracy not available to the traditional radiochemical method. This permitted the identification by mass and estimation of the yields of previously unknown nuclei like  $^{74}\text{Rb}$  and  $^{71}\text{Br}$ , which are close to the nucleon stability limit.<sup>9</sup> Later, other authors<sup>10</sup> confirmed the existence of the  $^{74}\text{Rb}$  isotope and measured its half-life ( $T_{1/2}=59$  msec).

The results of the mass-spectrometric measurements of the yields of the Rb and Br isotopes (see Fig. 2 and Table III) take into account corrections for the contribution of neighboring isobars and the fraction of Rb and Br isotopes that were able to decay during the extraction of the nuclei from the target, and also a correction for the dependence of the ion detection efficiency on the ion mass.

In the case of the copiously produced nuclides, the errors in the measurements of the relative yields of the Rb and Br isotopes were 2–4%, appreciably less than the er-



TABLE II. Even-odd isotope effect  $\Delta$  in the  $^{12,13}\text{C}(p, X)\text{Li}$  reaction at  $E_p=1$  GeV.

Reaction		$^{12}\text{C}(p, X)^{6-9}\text{Li}$	$^{13}\text{C}(p, X)^{6-9}\text{Li}$
Experiment		$0,54 \pm 0,13$	$0,44 \pm 0,04$
	[6]	0,32	-0,06
Calculation	[7]	0,70	-0,07
	[8]	0,30	0,04

Note. The calculations were based on the experimental data of Table I, and also the yields of lithium isotopes calculated in accordance with formulas taken from Refs. 6-8.

rors in the determination of the absolute values of the independent yields of these isotopes by means of gamma spectroscopy, which was carried out in order to normalize the mass-spectrometric data.

The absolute normalization of the yields of the Rb and Br isotopes was established by means of the monitor reaction  $^{27}\text{Al}(p, n3p)^{24}\text{Na}$  by measuring the intensities of the  $\gamma$  radiation of the corresponding nuclides by means of a Ge(Li) detector. For this, using deposition onto a substrate, we prepared special targets of enriched zirconium isotopes in the form of thin dioxide films (approximately 20 mg) attached under pressure to polystyrene films (thickness 0.2 mm). Aluminum monitor foils (thickness 10  $\mu\text{m}$ ) were placed on both sides of each zirconium target. All targets were irradiated simultaneously in the extracted proton beam, the integrated flux of which was  $4 \cdot 10^{15} \text{ cm}^{-2}$ . The amount of zirconium dioxide was determined by weighing the ash residue after combustion of the targets in a muffle furnace at  $T=900^\circ\text{C}$ .

From multiple measurements of the intensity of the  $\gamma$  radiation the activity was determined, and then also the total number of atoms of the corresponding nuclides produced in the target. The  $\gamma$  transitions were identified by their energies and the half-lives of the product nuclei. We measured the yields of 19 nuclides with  $71 \leq A \leq 89$ ; for seven nuclides, we were able to determine the independent

yields, and for the remainder the cumulative yields. The results of the measurements are given in Table III. The data take into account errors in the determination of the intensity of the proton beam, in the amount and uniformity of the deposited target material, and in the efficiency of the Ge(Li) detector; the total rms error is 6%.

The absolute normalization of the mass-spectrometric data on Rb, needed to determine the cross sections for production of the Rb isotopes, was found from the independent yields of  $^{83,84}\text{Rb}$  measured by means of the gamma spectrometer with error equal to 11%.

The absolute values of the Br isotope yields were determined by interpolating the independent yields of As and Rb.<sup>11,12</sup> At the same time, the results of the calculations of the yields of all the As, Br, and Rb isotopes were compared with the measured independent yields of  $^{72,74}\text{As}$  and  $^{83,84}\text{Rb}$ , and also with the curves of the relative yields of Br and Rb obtained by means of the mass spectrometer. The error in the determination of the cross sections for the production of Br isotopes in such a procedure was estimated at 20%.

To show the accuracy of the mass-spectrometric measurements of the relative yields of the Br or Rb isotopes for each target separately, the errors in the normalization of these data are not taken into account in the values given for the errors in the cross sections for production of the Br and Rb isotopes given in Table III.

The dependence of the yields of the Rb isotopes on the mass number  $A$  is close to the Gaussian curve (Fig. 2) for all targets:  $^{94}\text{Zr}$ ,  $^{91}\text{Zr}$ , and the "magic" nucleus  $^{90}\text{Zr}$ . However, it can be seen from Fig. 2 that on the transition from one target to another the curve of the yields of the Rb isotopes is somewhat transformed. At the same time, the total Rb yield remains constant within the errors, and one observes only a displacement of the centroid of the yield curve, which is, in fact, quite noticeable even for targets with mass number differing by unity.

The experimental values of the cross sections for the production of Rb isotopes with even and odd numbers of neutrons are systematically above and below the approximating curve of the type (1).

A similar effect is also observed in the yields of the bromine isotopes. If we consider the thermodynamic stage of evaporation, the magnitude of the even-odd effect  $\Delta$  in the yields of the product nuclei can be influenced by two factors that depend on the parity of the numbers of protons and neutrons.

The first factor is the difference in the density of levels  $\rho$  of the residual nuclei. This can be taken into account by introducing the parameter  $\delta$  in the expression

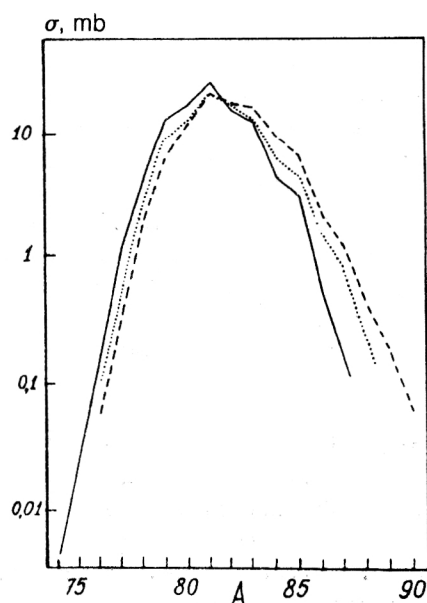


FIG. 2. Cross sections for production of rubidium isotopes in the  $\text{Zr}(p, 4pxn)\text{Rb}$  reaction at  $E_p=1$  GeV for different isotope targets (continuous line for  $^{90}\text{Zr}$ , dotted for  $^{91}\text{Zr}$ , and broken for  $^{94}\text{Zr}$ ).

TABLE III. Results of measurements of the cross sections for production of products of spallation of the  $^{90,91}\text{Zr}$  and  $^{94}\text{Zr}$  nuclei induced by 1-GeV protons (mb).

Gamma spectrometer				
Product	Target			
	$^{90}\text{Zr}$	$^{91}\text{Zr}$	$^{94}\text{Zr}$	
$^{71}\text{As}_{\text{cum}}$	$14 \pm 1$	$12,8 \pm 0,9$	$9,3 \pm 0,7$	
$^{72}\text{As}_{\text{ind}}$	$17 \pm 1$	$17 \pm 2$	$15 \pm 1$	
$^{74}\text{As}_{\text{ind}}$	$4,2 \pm 0,3$	$4,7 \pm 0,4$	$7,3 \pm 0,5$	
$^{72}\text{Se}_{\text{cum}}$	$5,5 \pm 0,5$	$4,1 \pm 0,4$	$3,1 \pm 0,3$	
$^{73}\text{Se}_{\text{cum}}$	$12,9 \pm 0,8$	$11,5 \pm 0,7$	$8,5 \pm 0,6$	
$^{75}\text{Se}_{\text{cum}}$	$24 \pm 2$	$23 \pm 2$	$20 \pm 2$	
$^{77}\text{Br}_{\text{cum}}$	$21 \pm 2$	$20 \pm 1$	$18 \pm 1$	
$^{81}\text{Rb}_{\text{cum}}$	$20 \pm 1$	$18 \pm 1$	$14,3 \pm 0,9$	
$^{82}\text{Rb}^*_{\text{ind}}$	$12 \pm 1$	$13 \pm 1$	$17 \pm 1$	
$^{83}\text{Rb}_{\text{ind}}$	$14 \pm 2$	$13 \pm 3$	$18 \pm 2$	
$^{84}\text{Rb}_{\text{ind}}$	$4,6 \pm 0,4$	$5,6 \pm 0,5$	$11,3 \pm 0,8$	
$^{82}\text{Sr}_{\text{cum}}$	$15 \pm 1$	$12 \pm 1$	$6,7 \pm 0,7$	
$^{83}\text{Sr}_{\text{cum}}$	$20 \pm 2$	$19 \pm 1$	$12,1 \pm 0,9$	
$^{86}\text{Y}_{\text{ind}}$	$24 \pm 2$	$21 \pm 1$	$15 \pm 1$	
$^{87}\text{Y}^*_{\text{cum}}$	$27 \pm 2$	$25 \pm 2$	$20 \pm 2$	
$^{87}\text{Y}^*_{\text{ind}}$	$(14 \pm 2)$	$(15 \pm 2)$	$(15 \pm 2)$	
$^{87}\text{Y}_{\text{ind}}$	$12 \pm 3$	$9 \pm 2$	$5 \pm 2$	
$^{88}\text{Y}_{\text{ind}}$	$27 \pm 2$	$25 \pm 2$	$25 \pm 2$	
$^{86}\text{Zr}_{\text{cum}}$	$6,3 \pm 0,4$	$4,6 \pm 0,4$	$1,6 \pm 0,2$	
$^{88}\text{Zr}_{\text{cum}}$	$27 \pm 2$	$20 \pm 1$	$10,8 \pm 0,8$	
$^{89}\text{Zr}_{\text{cum}}$	$45 \pm 3$	$29 \pm 2$	$17 \pm 1$	
Mass spectrometer				
A of product	$^{90}\text{Zr}(p,4pxn)\text{Rb}$	$^{91}\text{Zr}(p,4pxn)\text{Rb}$	$^{94}\text{Zr}(p,4pxn)\text{Rb}$	$^{91}\text{Zr}(p,6pxn)\text{Br}$
71	—	—	—	$0,04 \pm 0,04$
72	—	—	—	$0,3 \pm 0,1$
73	—	—	—	$0,5 \pm 0,1$
74	$0,006 \pm 0,006$	—	—	$3,7 \pm 0,4$
75	$0,013 \pm 0,005$	—	—	$10,7 \pm 0,3$
76	$0,13 \pm 0,03$	$0,19 \pm 0,08$	$0,1 \pm 0,1$	$14,1 \pm 0,4$
77	$1,19 \pm 0,04$	$0,4 \pm 0,1$	$0,3 \pm 0,1$	$16,0 \pm 0,6$
78	$4,4 \pm 0,2$	$2,5 \pm 0,2$	$2,0 \pm 0,2$	$10 \pm 1$
79	$13,2 \pm 0,4$	$8,9 \pm 0,4$	$6 \pm 1$	$(6 \pm 1)$
80	$17,7 \pm 0,9$	$12,7 \pm 0,6$	$12,5 \pm 0,8$	$3 \pm 1$
81	$26,4 \pm 0,9$	$21 \pm 1$	$22,5 \pm 0,9$	$(1,2 \pm 0,4)$
82	$15,7 \pm 0,4$	$18,1 \pm 0,8$	$19 \pm 1$	$0,4 \pm 0,2$
83	$12,5 \pm 0,5$	$12,2 \pm 0,6$	$18 \pm 2$	$0,3 \pm 0,2$
84	$4,3 \pm 0,3$	$6,3 \pm 0,4$	$11 \pm 1$	$0,05 \pm 0,05$
85	$3 \pm 1$	$4,5 \pm 0,8$	$6 \pm 2$	—
86	$0,45 \pm 0,05$	$1,6 \pm 0,4$	$2,3 \pm 0,3$	—
87	—	$0,9 \pm 0,4$	$1,3 \pm 0,2$	—
88	—	$0,2 \pm 0,1$	$0,4 \pm 0,2$	—
89	—	—	$0,2 \pm 0,1$	—
90	—	—	$0,07 \pm 0,07$	—

\*Isomer states  $^{82}\text{Rb}$  ( $E=100$  keV) and  $^{87}\text{Y}$  (381.3 keV).

Note. Values obtained by interpolating the yields of neighboring isotopes are given in brackets.

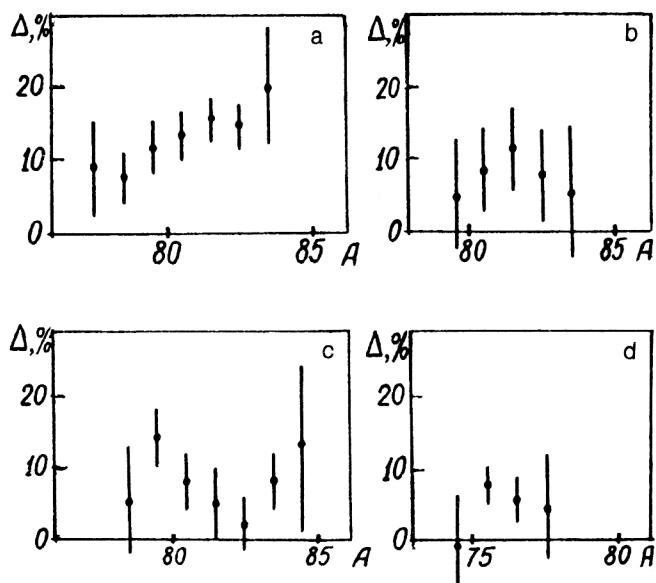


FIG. 3. Even-odd effect in different sections of the Rb and Br isotope yield curves: a) for yields of Rb from a  $^{90}\text{Zr}$  target; b) Rb from  $^{94}\text{Zr}$ ; c) Rb from  $^{91}\text{Zr}$ ; d) Br from  $^{91}\text{Zr}$ .

$$\rho \sim \exp[2\sqrt{a(E-\delta)}]. \quad (4)$$

It is assumed that  $\delta=0$  for odd-odd nuclei and  $\delta>0$  for all other nuclei.<sup>13</sup>

On the other hand, the value of  $\Delta$  is influenced by the factor representing the difference between the neutron binding energies of the product nuclei with even and odd numbers of neutrons. This factor tends to increase the probability for the production of nuclei with odd numbers of neutrons.

It is obvious that both these factors must have a particularly important influence in the final steps of the evaporation stage, when the excitation energy of the nucleus becomes comparable with the neutron binding energy. Our experimental data (Figs. 2 and 3), which exhibit a systematic excess of the independent yields of the Rb and Br isotopes with even numbers of neutrons, indicate that in the final steps in the stage of thermodynamic evaporation the dominant role is played by the difference in the binding energy of the evaporating neutron, which reaches 3 MeV, and not in the level density.

The reason for this is probably that when the nucleons evaporate from the compound nucleus the complete set of possible states is not realized; the only states of the nuclei are limited in number and especially selected in their nature. A similar effect is also observed in neutron spectroscopy in the  $(n,\gamma)$  reaction, for which the  $\gamma$  cascades do not proceed through all possible intermediate states.<sup>14</sup>

A connection between the even-odd effect and the properties of the residual nuclei in the reactions is also indicated by the presence of a dependence of the magnitude of the effect on the loss of nucleons, i.e., on the mass difference of the product nuclei and the target nuclei. Such a dependence is shown in Fig. 4 for the zirconium spallation reaction. The values of  $\Delta$  given in this figure were obtained

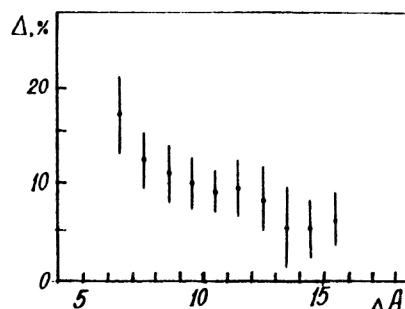


FIG. 4. Dependence of the even-odd isotope effect on the loss of nucleons in spallation of Zr nuclei.

by averaging the data for all the investigated reactions on zirconium. The decrease in the magnitude of  $\Delta$  with increasing loss of nucleons is explained by the fact that there is then an increase in the mean excitation energies corresponding to them and in the angular momentum of the residual nuclei. In turn, this leads to a growth in the kinetic energy of the evaporating particles, to an increase in the probability of excitation of collective degrees of freedom of the residual nuclei, and, therefore, to a decrease in the effect of the pairing correlations of the nucleons in these nuclei.

#### PROTON-INDUCED FISSION OF $^{238}\text{U}$ . ISOTOPIC EFFECTS

The mass spectrometer "in line" with the accelerator was used to measure the relative yields of the isotopes  $^{79-97}\text{Rb}$  and  $^{121-146}\text{Cs}$  resulting from  $^{238}\text{U}$  fission induced by protons with  $E_p=1$  GeV.<sup>15</sup> To determine more accurately the nature of the dependence of the form of the isotope distributions of the fragments on  $E_p$ , we also measured the yields of the isotopes  $^{81-94}\text{Rb}$  at  $E_p=750$  MeV.<sup>16</sup> The mean time of extraction of the Rb and Cs atoms from the target was 30–50 msec. In the measured line intensities of the mass spectra, corrections were introduced for the radioactive decay of the product nuclei within the target, for the partial ionization of the Sr and Ba isotopes, and for the ion mass discrimination in the detector. The total magnitude of the corrections did not exceed 3% for Rb and 6% for Cs.

The results of the measurements are presented in Table IV and in Figs. 5–7 with the error of only the relative measurements of the yields of the Rb and Cs isotopes in the mass spectrometer without allowance for the errors in their normalization. To obtain the absolute normalization of the measured Rb and Cs isotope distributions, we used the results of Ref. 17. In the data for  $E_p=1$  GeV, the error in the absolute values of the fragment yields was 13% for Rb and 7.5% for Cs. To normalize the Rb isotope distribution obtained at  $E_p=750$  MeV, we interpolated the absolute yields of  $^{84}\text{Rb}$  and  $^{86}\text{Rb}$ , measured in the study of Ref. 17 at  $E_p=0.68$  and 1.0 GeV. For the normalization, we used the sum of the interpolated estimates of the  $^{84}\text{Rb}$  and  $^{86}\text{Rb}$  yields for  $E_p=0.75$  GeV, which were taken to be 4.4 and 8.9 mb, respectively.

TABLE IV. Cross sections for production of Rb and Cs isotopes resulting from <sup>238</sup>U fission induced by protons with E<sub>p</sub>=750 MeV and 1 GeV (mb).

A <sub>Rb</sub>	E <sub>p</sub> = 750 MeV	E <sub>p</sub> = 1 GeV	A <sub>Cs</sub>	E <sub>p</sub> = 1 GeV
79	—	0,10 ± 0,3	121	0,12 ± 0,06
80	—	0,23 ± 0,03	122	0,21 ± 0,08
81	0,6 ± 0,2	0,9 ± 0,1	123	0,6 ± 0,1
82	1,4 ± 0,3	2,2 ± 0,1	124	0,8 ± 0,1
83	2,9 ± 0,6	4,3 ± 0,1	125	1,6 ± 0,2
84	4,2 ± 0,9	7,0 ± 0,1	126	2,1 ± 0,2
85	7,5 ± 0,9	9,6 ± 0,8	127	3,2 ± 0,3
86	9 ± 1	10,1 ± 0,2	128	3,8 ± 0,2
87	9 ± 1	9,6 ± 0,4	129	4,9 ± 0,2
88	10 ± 2	9,0 ± 0,2	130	4,8 ± 0,3
89	11 ± 1	9,2 ± 0,1	131	5,4 ± 0,2
90	11,8 ± 0,9	9,3 ± 0,1	132	5,3 ± 0,2
91	9,5 ± 0,8	7,9 ± 0,1	133	5,1 ± 0,3
92	8,3 ± 0,8	5,05 ± 0,07	134	4,3 ± 0,2
93	4,6 ± 0,6	3,46 ± 0,07	135	4,1 ± 0,2
94	2,6 ± 0,5	1,9 ± 0,1	136	4,0 ± 0,2
95	—	0,94 ± 0,08	137	4,8 ± 0,3
96	—	0,37 ± 0,08	138	3,6 ± 0,3
97	—	0,17 ± 0,05	139	4,5 ± 0,3
			140	2,5 ± 0,3
			141	1,8 ± 0,2
			142	1,0 ± 0,2
			143	0,51 ± 0,07
			144	0,22 ± 0,06
			145	0,12 ± 0,06
			146	0,06 ± 0,04

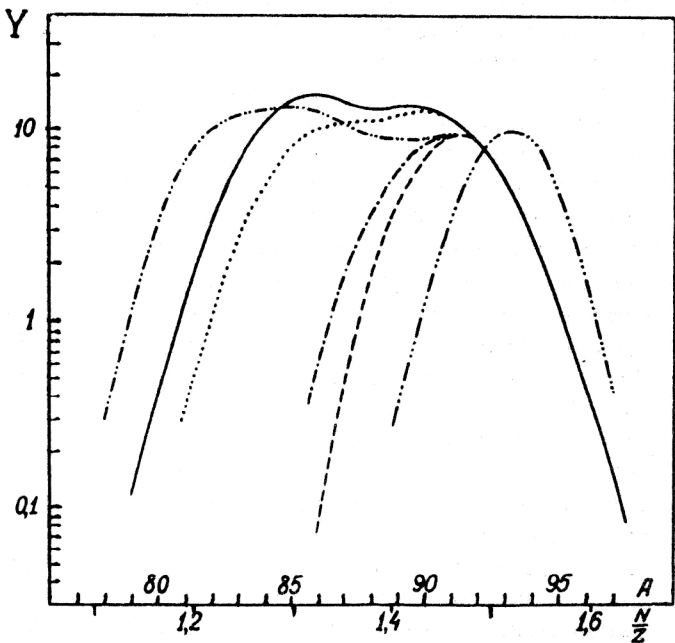


FIG. 5. Distribution of yields of Rb isotopes (in relative units) produced by <sup>238</sup>U fission induced by reactor neutrons (Ref. 19, triple dash-dot chain curve) and also by protons with energy 40 MeV (Ref. 2, broken curve), 100 MeV (Ref. 20, chain curve), 1 GeV (continuous curve), 0.75 GeV (dotted curve), and 24 GeV (Ref. 21, double dash-dot chain curve). The curves for protons are normalized by the sum of the <sup>91-97</sup>Rb yields, and the curve for neutrons by the total yield of all Rb isotopes, using the data for E<sub>p</sub>=40 MeV.

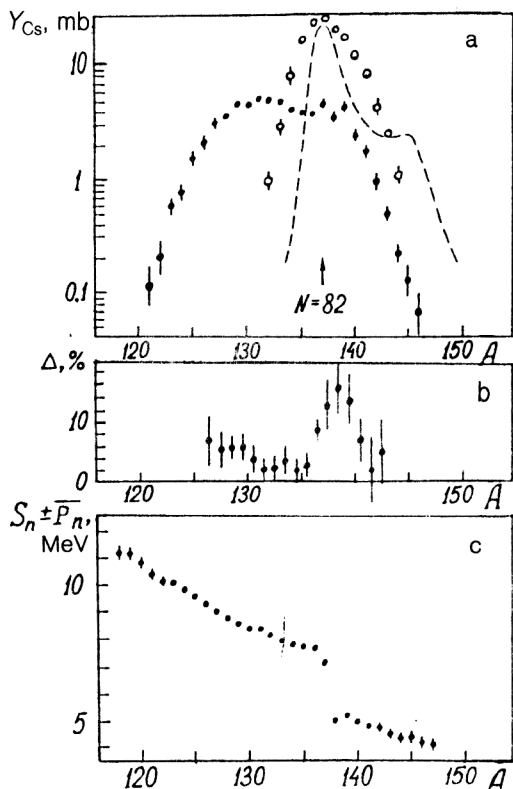


FIG. 6. a) Cross sections for production of Cs isotopes resulting from  $^{238}\text{U}$  fission induced by protons with  $E_p=60$  MeV (open circles) and  $E_p=1$  GeV (black circles). The broken curve gives the results of a calculation in accordance with a modified statistical model at nuclear temperature  $T=2$  MeV. b) The magnitude  $\Delta$  of the even-odd effect. c)  $S_n \pm \bar{P}_n$ , the binding energy of one neutron, corrected for the pairing energy.

In the study of Ref. 18 of the same group of Rb and Cs isotopes, their masses were determined experimentally to a good accuracy, using a mass spectrometer with resolution  $R=5000$ . Comparison of these data with the isotope distributions of the fragments makes it possible to investigate the isotopic effects in their yields associated with the structure of the nuclei, namely, pairing effects and the filling of subshells and shells.

In Figs. 6a and 7a we compare data for the independent yields of the fragment products  $Y_{\text{Rb}(\text{Cs})} = f(A_{\text{Rb}(\text{Cs})})$  in the case of uranium fission induced by protons with  $E_p=60$  MeV and  $E_p=1$  GeV. At energy  $E_p=1$  GeV, the function  $f(A_{\text{Rb}(\text{Cs})})$  acquires a two-hump form with fine-structure elements, this being due to the addition of a group of relatively neutron-deficient isotopes. When a nuclear shell is closed, the resulting configurations of the nuclei are most stable and have minimal potential energy, and therefore in nuclear reactions the production of nuclei with magic numbers of nucleons, for example,  $N=50, 82$ , is energetically more advantageous. The possible occurrence of such shell effects is also indicated by calculations<sup>22</sup> in accordance with a modified statistical model (Figs. 6a and 7a). However, it is obvious that the comparatively high mean excitation energy ( $E^* \approx 200$  MeV) will lead to a growth in the dispersion of the isotope distributions and a

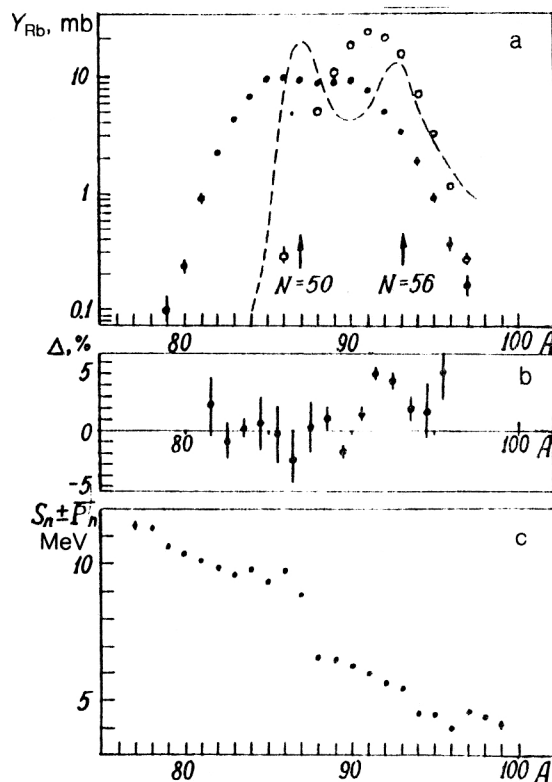


FIG. 7. a) Cross sections for production of Rb isotopes resulting from  $^{238}\text{U}$  fission induced by protons with  $E_p=60$  MeV (open circles) and  $E_p=1$  GeV (black circles). The broken curve gives the results of a calculation in accordance with the modified statistical model at nuclear temperature  $T=2$  MeV. b) The magnitude  $\Delta$  of the even-odd effect. c)  $S_n \pm \bar{P}_n$ , the binding energy of one neutron, corrected for the pairing energy.

smoothing of their two-hump structure, as is observed in the experiments.

It is interesting to note that the accurate measurements of  $Y_{\text{Rb}(\text{Cs})} = f(A_{\text{Rb}(\text{Cs})})$  make it possible to detect the manifestation of the even more subtle isotopic effects of neutron pairing. To demonstrate this, we use, as before, a Gaussian to approximate the sections of the curve for groups of four nuclides and we calculate the deviations of the cross sections from the smooth curve (the even-odd effect), obtaining  $\Delta$  in accordance with the formula (3).

It can be seen in Figs. 6b and 7b that the values of  $\Delta$  as functions of  $A$  exhibit a systematic excess of the probability for the production of isotopes with even numbers of neutrons, i.e., for the fragment products there also exists an even-odd effect associated with neutron pairing. This is revealed especially clearly for the cesium isotopes, for which, for several reasons, the accuracy in the determination of  $\Delta$  is higher. In the case of cesium there is an increase in the value of  $\Delta$  in the region of  $A=137$ , and for rubidium there is one in the region of  $A \approx 93$ . In the first case, the pairing effect is enhanced because the  $N=82$  structure is magic, and in the second case it is enhanced by the closing of the neutron subshell  $d_{5/2}$  ( $N=56$ ). One may suppose that the influence of this neutron subshell is strengthened by the influence of the proton subshell



$f_{5/2}$  ( $Z=38$ ), since the charge for the rubidium isotopes,  $Z_{\text{Rb}}=37$ , is close to the charge of this closed subshell, and the combined effects of the two factors raise the probability for the production of rubidium isotopes in the region of  $A=92-93$ . From the experimentally known masses of the rubidium and cesium isotopes, we can calculate the neutron pairing energy:

$$P_n = \frac{(-1)^N}{4} [2 \cdot S_n(N, Z) - S_n(N+1, Z) - S_n(N-1, Z)], \quad (5)$$

where  $S_n$  is the neutron binding energy.

The difference between the neutron binding energies for nuclei with odd and even numbers of neutrons can be characterized by the averaged quantity  $\bar{P}_n$ . It can be seen from Figs. 6c and 7c how  $S_n$ , the binding energy of one neutron, smoothed by the amount  $\pm \bar{P}_n$  ( $-\bar{P}_n$  and  $+\bar{P}_n$ , respectively, for even and odd  $N$ ), changes with the isotope mass.

It follows from comparison of Figs. 6b, 7b and Figs. 6c, 7c that the additional growth of the binding energy in the region of the subshells and shells leads to an increase of the independent yields of the corresponding isotopes. In the case of rubidium, the lower accuracy in the determination of the independent yields (the natural admixtures of the stable isotopes  $^{85,87}\text{Rb}$  present problems), and also the complicated dependence  $Y_{\text{Rb}} = f(A_{\text{Rb}})$  make it impossible to draw a definite conclusion about the influence of pairing energy on the values of the cross sections in the region of the  $N=50$  shell.

It should be emphasized that the complete set of experimental results confirms a remarkable circumstance, namely, the manifestation of the magic condition and the effect of pairing in the process of production of fission fragments resulting from the interaction of intermediate-energy protons with uranium nuclei. Thus, the accurate measurements of the yields of the reaction products, like the measurements of the nuclide masses, provide information about new regions of deformation and sphericity of the nuclides.<sup>23</sup>

It is obvious that the even-odd effect arises mainly at minimum excitation energies  $E^*$ , i.e., when the last neutrons evaporate, since the difference between the binding energy of odd and even neutrons (1–2 MeV) is too slight and can hardly have a significant influence at large  $E^*$ . We also emphasize that in the process of thermodynamic evaporation of nucleons from the fission fragments the factor represented by the difference between the neutron binding energies plays a more important role than the factor represented by the level densities, since in the case of the rubidium and cesium isotopes with odd numbers of neutrons the cross sections for their production are, despite the high level density in them, lower on the average than for the isotopes with even numbers of neutrons (see Figs. 6b and 7b).

In order to investigate the mechanism of high-energy fission, we analyzed the change in the shape of the isotope distributions of the fragments as the energy of the protons

that induced the  $^{238}\text{U}$  fission was increased from 30 MeV to 24 GeV.

The yield distributions of the Rb isotopes resulting from  $^{238}\text{U}$  fission induced by protons of different energies are shown in Fig. 5.

It should be noted that in the region of intermediate energies ( $\sim 1$  GeV) the mass-spectrometric experimental data needed for such analysis were not available. This gap was filled after the measurements had been made of the yields of Rb and Cs isotopes resulting from  $^{238}\text{U}$  fission induced by protons with  $E_p=0.75$  and 1.0 GeV.<sup>15,16</sup> We shall consider only these product nuclei, since Rb and Cs are some of the most probable representatives of the light and heavy fragments resulting from fission of uranium induced by particles of any energy. It can therefore be assumed that their isotope distributions are typical and reflect the main features in the dependence of the nucleon composition of the fragments on the proton energy. The experimental data made it possible to establish that as  $E_p$  is increased in the region of 1 GeV the isotope distributions of the fragments abruptly become broader for both the heavy and light fragments. Moreover, the broadening is due to a growth in the yields of the neutron-deficient Rb and Cs isotopes, and the shape and position of the neutron-rich wing of the isotope distributions of these fragments remain practically unchanged. As a result, already at  $E_p=1$  GeV the distributions acquire a two-hump form with a small minimum in the region of the stable isotopes. The further increase of  $E_p$  from 1 to 24 GeV did not lead to a significant change in the shape of the isotope distributions of the fragments and merely slightly shifted and broadened the neutron-deficient hump in the direction of smaller  $N/Z$ .

For the mass spectrometer "in line" with the accelerator, the detection of the product nuclei is done inclusively and does not depend on the types of reactions that result in the production of the studied nuclides. Therefore, we made only an estimate of the contribution of the nonfission processes to the measured yields of the Rb and Cs isotopes at  $E_p=1$  GeV. The estimate was based on comparison of the total yields of the isobars with  $A=88$  and 133, which were determined in one case after extrapolation of the Rb and Cs isotope distributions to their neighboring elements, and in another case from the fragment mass distribution obtained by other authors who selected events corresponding to binary fission of the residual nuclei.<sup>24</sup> The isobar yields obtained by the two methods agreed within the errors of the measurements, which were 10–15%, from which it was concluded that the contribution of the nonfission events to the Rb and Cs yields was small, and that they could not be responsible for the appearance of the neutron-deficient group of fragments, which contained 60–65% of all the produced Rb and Cs isotopes.

Although the most probable  $N/Z$  values of the fragments vary strongly with the nucleon composition and the excitation energy of the original nuclei (see Fig. 8), the difference between these values for the additional fragments depends very weakly on the energy and the parameters of the fissioning nuclei and is determined solely by the

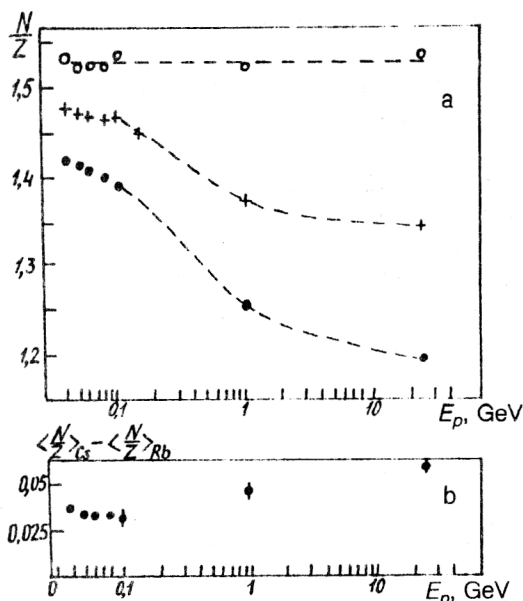


FIG. 8. Nucleon composition of fragments resulting from  $^{238}\text{U}$  fission as a function of the energy of the incident proton: a) The relative nucleon content in the Rb isotopes corresponding to the centroid (+) and the half-maximum of the neutron-rich (open circles) and neutron-deficient (black circles) wings of the Rb isotope distributions. The experimental points are connected for clarity. b) Difference between the positions of the centroids of the Rb and Cs isotope distributions. Data from Refs. 2, 15, 20, 21, and 39 were used.

ratio of the fragment masses. In this connection, it was conjectured that the mechanism of distribution of the charges between the fragments remains practically unchanged in a large range of energies of the protons that induce the uranium fission, including  $E_p = 1$  GeV. This means that the factors that influence the width and position of the isotope distributions of the fragments can be divided into two groups. One of them is related directly to the statistical nature of the process of division of charge between the fragments at the time of fission and determines the dispersion of the charges of the primary fragments. The other group of factors characterizes the differences between the fissioning nuclei as regards the nucleon composition and the excitation energy. This last effect leads to a shift and broadening of the isotope distributions of the fragments, which, ultimately, are the result of the superposition of a large number of partial distributions of normal form corresponding to different fissioning nuclei.

### LOSSES OF NUCLEONS AND CHARGE PER $^{238}\text{U}$ FISSION EVENT

The direct measurement of the loss of nucleons by simultaneous detection of all the particles produced as a result of interaction of high-energy protons with nuclei is a very complicated technical problem. A more realistic method of solving the problem is to measure the masses  $M_1$  and  $M_2$  and charges  $Z_1$  and  $Z_2$  of both fragments. For a  $^{238}\text{U}$  target, we determine the loss of nucleons and charge as follows:

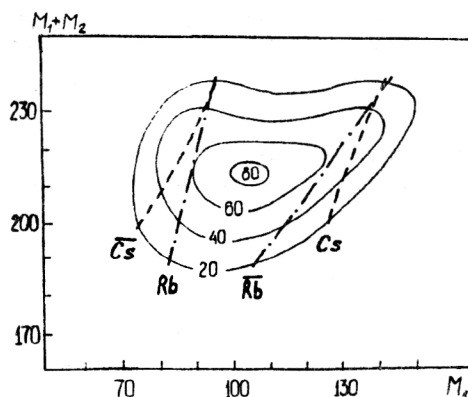


FIG. 9. Contour diagram of mass correlations of complementary fragments resulting from  $^{238}\text{U}$  fission induced by 1-GeV protons. The broken and chain curves show the most probable masses of the Rb and Cs fragments and also their complementary fragments, denoted nominally as  $\bar{Rb}$  and  $\bar{Cs}$ .

$$\Delta A = 238 - M_1 - M_2, \quad (6)$$

$$\Delta Z = 92 - Z_1 - Z_2. \quad (7)$$

There exists a possibility of experimental determination of the loss of nucleons and charge resulting from fission of nuclei induced by high-energy protons by joint analysis of the results of the two experiments. Use is made here of the high accuracy in the determination of the isotope composition of the fragments in the mass spectrometer (the connection between the  $Z$  and  $M$  of the fragments), and also the correlation between  $M_1$  and  $M_2$ , which is established by means of a two-arm time-of-flight spectrometer.<sup>24,25</sup>

Comparison of the Rb and Cs isotope distributions with the mass distributions of the complementary fragments obtained in Ref. 24 from  $^{238}\text{U}$  fission introduced by protons with  $E_p = 1$  GeV made it possible to determine the most probable masses and charges of the fragments that were complementary for Rb and Cs. It also proved possible to establish the dependence of the loss of nucleons and charge per  $^{238}\text{U}$  fission event on the  $N/Z$  ratio of the product nuclei, this being due to the fact that neutrons represent the main fraction of the losses. The nucleon and charge losses were determined for three characteristic  $N/Z$  values of the Rb and Cs fragments corresponding to the half-maximum and centroid of the isotope distributions of these fragments. The contour diagram of the masses of the complementary fragments taken from Ref. 24 was used in this work.

We first calculated the most probable nucleon losses for Rb and Cs fragments with the mean mass values  $\langle M_{Rb} \rangle$  and  $\langle M_{Cs} \rangle$  of these fragments. From the contour diagram shown in Fig. 9, we determined the mass distributions of the complementary fragments for values of  $M_1$  equal to  $\langle M_{Rb} \rangle$  and  $\langle M_{Cs} \rangle$ . As the most probable masses of the complementary fragments we took the weighted mean values of  $M_2$  in these distributions. Here and in what follows, it is assumed that the shape of the isotope distributions of

TABLE V. Loss of nucleons  $\Delta A$  and of charge  $\Delta Z$  per  $^{238}\text{U}$  fission event induced by high-energy protons resulting in the production of Rb or Cs fragments (for the notation, see the text).

Energy	$E_p = 1 \text{ GeV}$		$E_p = 11 \text{ GeV}$
	Rb	Cs	Rb
$M_{1,\text{def}}$	$83,3 \pm 0,2$	$126,4 \pm 0,2$	80,5
$\Delta A_{\text{def}}$	$45 \pm 2$	$35 \pm 3$	72
$\Delta Z_{\text{def}}$	$6,8 \pm 0,9$	$2,6 \pm 1,2$	16
$\langle A \rangle$	$87,79 \pm 0,04$	$133,09 \pm 0,09$	86,5
$\Delta A_{\text{av}}$	$26,4 \pm 0,5$	$18,2 \pm 0,4$	36
$\Delta Z_{\text{av}}$	$3,6 \pm 0,3$	$1,3 \pm 0,5$	7
$M_{1,\text{rich}}$	$92,1 \pm 0,2$	$139,5 \pm 0,2$	93,5
$\Delta A_{\text{rich}}$	$7,8 \pm 0,5$	$6,9 \pm 0,8$	8,5
$\Delta Z_{\text{rich}}$	$0,4 \pm 0,3$	$-0,1 \pm 0,4$	0,2

the neighboring elements of Rb and Cs is the same. The average nucleon loss was found from the expression

$$\Delta A_{\text{av}} = 238 - \langle M_{\text{Rb(Cs)}} \rangle - \langle M_2 \rangle. \quad (8)$$

To estimate the average charge loss for  $^{238}\text{U}$  fission events with the production of Rb or Cs, it was necessary to determine the most probable charge of the fragments complementary for Rb and Cs, the mean mass of which was found from the contour diagram. Here, we took into account the fact that the mean value of  $N/Z$  of the fragments varies weakly with their mass,<sup>26</sup> and that the masses of the fragments complementary for Rb are close to the mean mass of the Cs fragments, and  $\langle M_2 \rangle_{\text{Cs}}$  are close to  $\langle M_{\text{Rb}} \rangle$ . Therefore, in calculating the estimates it is acceptable to assume a linear approximation for the dependence of the nucleon composition of the fragments on their mass. The coefficients of this dependence were determined from the mean values of  $N/Z$  for the Rb and Cs fragments measured by the mass spectrometer "in line" with the accelerator:  $\langle (N/Z)_{\text{Rb}} \rangle = 1.373 \pm 0.001$  and  $\langle (N/Z)_{\text{Cs}} \rangle = 1.420 \pm 0.002$ . Using these values, we found the relationship between the mean value of  $N/Z$  of a contemporary fragment and its mass:

$$\langle (N/Z)_2 \rangle = 1.282 + 0.00104 \langle M_2 \rangle. \quad (9)$$

The mean charge loss in the case of  $^{238}\text{U}$  fission with the production of Rb or Cs fragments was determined from the expression

$$\Delta Z_{\text{av}} = 92 - Z_{\text{Rb(Cs)}} - \langle M_2 \rangle / [\langle (N/Z)_2 \rangle + 1]. \quad (10)$$

In a similar manner we estimated the nucleon and charge losses for uranium fission events resulting in the production of neutron-deficient and neutron-rich Rb and Cs isotopes corresponding to the half-maximum of their isotope distributions shown in Figs. 6 and 7. For the masses of these fragments, denoted, respectively, by  $M_{1,\text{def}}$  and  $M_{1,\text{rich}}$ , we determined from the contour diagram (Fig. 9) the distributions of the total mass  $M_1 + M_2$ . For the mass of the fragment complementary for  $M_{1,\text{def}}$  we took the smaller of the two values of  $M_2$  corresponding to the half-

maximum of these distributions, and for  $M_{1,\text{rich}}$  we took the larger. The nucleon and charge losses for the neutron-deficient and neutron-rich fragments were calculated under the same assumptions as in the case of the average values, i.e., from formulas analogous to (8)–(10). The results of these calculations are given in Table V.

This table gives the nucleon and charge losses obtained in  $^{238}\text{U}$  fission events when one of the fragments was Rb or Cs. As can be seen from Table V, only neutron-rich Rb and Cs isotopes can be regarded as the most probable complementary fragments. The nucleon losses corresponding to these isotopes are 7–8 a.m.u., i.e., they are close to the mean losses characteristic for  $^{238}\text{U}$  fission induced by protons with energy 40–50 MeV.<sup>2</sup>

The method proposed here for determining the nucleon and charge losses on fission can also be used at other proton energies. As an example, Table V give estimates of the nucleon and charge losses for  $^{238}\text{U}$  fission obtained by analyzing data on the Rb isotope distribution at  $E_p = 10.5 \text{ GeV}$  (Ref. 27) and the contour diagram of the masses of the complementary fragments at  $E_p = 11.5 \text{ GeV}$  taken from Ref. 25.

Up to now in this section we have considered only  $^{238}\text{U}$  fission events for which one of the fragments was Rb or Cs. However, there is also interest in estimating the mean charge loss for all fission events. Such an estimate could be compared with data on the multiplicity of the charged particles in these reactions. However, since the isotope distributions of only Rb and Cs were measured by the mass spectrometer "in line" with the accelerator, to go over to such an estimate it is necessary to extrapolate the most probable values of the ratio of the numbers of neutrons and protons in the Rb and Cs fragments to other fragments. Here, it is necessary to take into account the difference in the ratio of the contributions of low-energy and high-energy fission in the yields of fragments with different values of the mass number. This difference leads to a certain difference in the shape of the isotope distributions and in the most probable values of  $N/Z$  for fragments with different  $Z$ .

In the behavior of the ratio  $N/Z$  of the fragments as a function of  $A$  given in Ref. 26 one may see that a small excess of  $N/Z$  over the very flat line is observed for fragment masses that coincide with the position of the peaks of asymmetric uranium fission that are characteristic for low excitation energies of the residual nuclei. If we exclude from the yields of all fragments the contribution of low-energy fission, then the dependence of the most probable values  $\langle N/Z \rangle_{pr}$  for the remaining part of the yields of the fragments on their mass number will be much more nearly linear than in the case of the mean values of  $N/Z$ . Finding this dependence from the two values of  $\langle N/Z \rangle_{pr}$  for the Rb and Cs isotopes produced in high-energy fission, and having estimated the common contribution of the low-energy component of the uranium fission, we can calculate the mean charge losses for all fission events.

In decomposing the Rb and Cs isotope distributions, we assume that the low-energy part of these distributions has the same values of the half-width and centroid position as for the total isotope distributions of the considered  $^{238}\text{U}$  fragments resulting from fission induced by protons with  $E_p=40$  MeV (Ref. 2). By the high-energy part of the Rb and Cs isotope distributions at  $E_p=1$  GeV we shall understand the residue after the low-energy part has been subtracted from the total distributions of these fragments. The normalization of the low-energy part of distributions obtained at different proton energies should be made using the sum of the yields of the most neutron-rich isotopes produced in fission events of residual nuclei with minimum excitation energy.

As a result of such a decomposition it was found that the contribution of low-energy uranium fission to the yields of the Rb isotopes is about 30% (28 mb), and for the Cs yields it is 36% (25 mb). The agreement of the estimates of the yields of the Rb and Cs isotopes corresponding to low-energy fission, which are the most probable complementary fragments, indicates that the normalization of the Rb and Cs yields at  $E_p=1$  GeV made using the data taken from Ref. 17 is reliable.

For the high-energy parts of the Rb and Cs isotope distributions from  $^{238}\text{U}$  fission induced by protons with  $E_p=1$  GeV, we determined the weighted means  $\langle N/Z \rangle_{pr}$  and from them found the dependence of this quantity on the mass number of the fragments:

$$\langle N/Z \rangle_{pr} = 1.25 + 0.00095A. \quad (11)$$

By means of this relation and the mass distribution of the fragments for the high-energy component of uranium fission given in Ref. 24, we determined the mean charge of these fragments, which was found to be  $\langle Z_{pr} \rangle = 44.1 \pm 0.8$ .

According to the estimate made in Ref. 24 using the contour diagram of the masses of the complementary fragments, the common contribution of the low-energy component of  $^{238}\text{U}$  fission to the yields of all fragments is about 10%. We obtained a similar estimate from the mass-spectrometric data on the Rb and Cs isotope distributions at  $E_p=1$  GeV. For this, from the low-energy part of these distributions, we determined the yields of isobars with mass equal to the most probable mass of the Rb or Cs

isotopes at  $E_p=40$  MeV, i.e., for  $A=91.5$  and 138. The total yield of these isobars was found to be  $21 \pm 2$  mb. From these data, taking into account the shape of the fragment mass distribution for  $E_p=32$  MeV (Ref. 28), we calculated the total yield of fragments corresponding to the low-energy component of  $^{238}\text{U}$  fission at  $E_p=1$  GeV, which was  $230 \pm 40$  mb. Bearing in mind that the  $^{238}\text{U}$  fission cross section at this proton energy is  $1470 \pm 70$  mb (Ref. 29), the fraction of the low-energy component is found to be  $15.6 \pm 3.5\%$ . This value is somewhat above the graphical estimate obtained in Ref. 24. As the true value it is reasonable to take the mean of these two estimates:  $P_{le}=13\%$ .

The average charge loss per  $^{238}\text{U}$  fission event at  $E_p=1$  GeV with allowance for the charge of the projectile proton was obtained in accordance with the formula

$$\Delta Z_{av}^{(1)} = (1 - P_{le})(92 - 2\langle Z_{pr} \rangle) + 1. \quad (12)$$

The value of  $\Delta Z_{av}^{(1)}$  was found to be  $4.3 \pm 1.5$ , in reasonable agreement with the results of calculations of the multiplicity of charged particles made in Ref. 30 and also with linear extrapolation of the experimental multiplicities of charged particles obtained at  $E_p=140$ , 460, and 660 MeV.<sup>31</sup>

## ISOTOPE DISTRIBUTIONS IN $\text{Ir}(p,X)\text{Rb}$ , $\text{Sr}$ , $\text{Cs}$ , $\text{K}$ REACTIONS

The investigation of uranium fission induced by protons with energy  $E_p=11.5$  GeV made in the study of Ref. 25 with a two-arm time-of-flight spectrometer led to the detection of a group of fragments corresponding to events with very high nucleon loss  $\Delta A = A_{tar} - A_1 - A_2 \cong A_{tar}/2$  and distinguished by a kinetic energy higher than predicted by the liquid-drop model. Fragments with unusual ratios of their kinetic energies and momenta were also observed in  $^{238}\text{U}$ ,  $^{232}\text{Th}$ , and  $^{197}\text{Au}$  fission induced by protons with  $E_p=1$  GeV.<sup>32,33</sup>

To explain this phenomenon, Wilkins *et al.*<sup>25</sup> suggested a new mechanism of production of such fragments, invoking the coherent-tube model to describe the initial interaction of the proton with the target nuclei. It was shown in Ref. 34 that such a reaction mechanism, with allowance for the effects of nuclear viscosity, makes it possible to explain qualitatively the anisotropy of the angular distributions of the heavy fragments and other fragments at different energies of the incident protons and product nuclei. In accordance with this mechanism, the nuclei fission during the fast stage of the reaction before thermodynamic equilibrium is established, since the spectator nuclear remnant is very unstable and rapidly breaks up into parts. For a central collision of a proton with target nuclei, there can be division into two fragments with approximately equal masses ( $A_1 \cong A_2$ ).

It is assumed in Refs. 25 and 35 that such fragments have a low excitation energy, and therefore the ratio of the neutrons and protons in them must be approximately the same as for the target nuclei. Therefore, in events of such pre-equilibrium fission more neutron-rich product nuclei

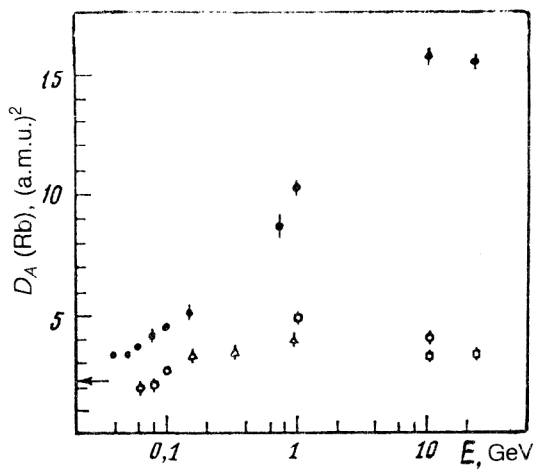


FIG. 10. Dispersion of Rb isotope distributions as a function of the energy of the projectile particles in the following reactions:  $^{238}\text{U}(p,X)\text{Rb}$  (Refs. 2, 15, 16, 20, 27, and 39–40, black circles),  $\text{Ir}(p,X)\text{Rb}$  (Refs. 36 and 37 and present study, open circles),  $\text{Ta}(p,X)\text{Rb}$  (Refs. 36 and 40, open squares), and  $\text{Ta}(^{12}\text{C},X)\text{Rb}$  (Ref. 40, open triangles). The arrow shows the value of  $D_A(\text{Rb})$  in the  $^{235}\text{U}(n_T,X)\text{Rb}$  reaction.<sup>41</sup>

must be produced than in the case of the ordinary mechanism of fission after an intranuclear cascade. Thus, if a reaction channel corresponding to the new fission mechanism opens when  $E_p$  is increased, this may affect the shape of the isotope distributions of the fragments. In the present investigation, we set ourselves the task of finding traces of such a reaction channel in the ratio of the cross sections for the production of fragments with different values of  $N/Z$  measured in the case of interaction of heavy nuclei with high-energy protons.

Because of the appreciable contribution of the low-energy fission component, the search for events corresponding to pre-equilibrium fission in the inclusive isotope distributions of the fragments is very difficult in the case of a uranium target. For this, it is necessary to make an additional selection of events using kinematic relations.

The situation becomes much simpler if as the target one chooses lighter nuclei, for example, iridium, for which the fission barrier is almost four times higher than for uranium. Data obtained earlier at  $E_p=10.5$  GeV (Ref. 36) and  $E_p=62, 80$ , and  $95$  MeV (Ref. 37) indicate that the isotope distributions of Rb fragments resulting from Ir fission induced by protons in a wide range of  $E_p$  can be well approximated by a Gaussian function. Moreover, as can be seen from Fig. 10, their width, in contrast to the data for the uranium target, increases very weakly with increasing  $E_p$ . At the same time, the position of the centroid of these distributions is shifted significantly into the neutron-deficient region from  $A_{\text{av}}(\text{Rb})=88.2$  at  $E_p=62$  MeV to  $A_{\text{av}}=82.1$  at  $E_p=10.5$  GeV, and this facilitates the search for traces of the new fission mechanism in the yields of neutron-rich fragments.

Such behavior of the isotope distributions of the fragments can be explained in the framework of the cascade-evaporation model of proton interaction with target nuclei by the increase in the mean excitation energy of the fis-

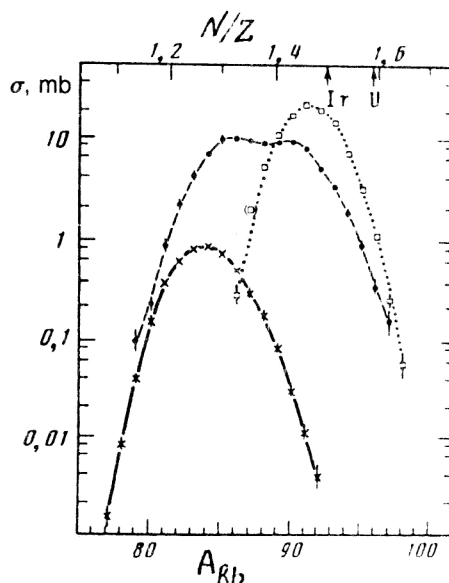


FIG. 11. Cross sections for production of Rb isotopes resulting from  $^{238}\text{U}$  fission induced by protons with  $E_p=60$  MeV (Ref. 2, open squares) and with  $E_p=1$  GeV (Ref. 15, black circles), and also from fission of Ir (natural) induced by protons with  $E_p=1$  GeV (crosses). The arrows indicate the mean  $N/Z$  values of the target nuclei.

sioning nuclei resulting from the increased number of cascade particles. Interesting objects for a search for effects associated with pre-equilibrium fission of Ir nuclei are Rb isotopes with  $A=87-93$ , which correspond to fission events with low emission of neutrons from the residual nuclei and fragments, since the value of  $N/Z$  for  $^{92}\text{Rb}$  and  $^{93}\text{Rb}$  is approximately the same as for the target nuclei (see Fig. 11). In the case of the ordinary mechanism of fission of Ir, the contribution of these isotopes to the total Rb yield must fall sharply with increasing  $E_p$ . Unfortunately, in the studies of Refs. 27 and 36 the yields of Rb isotopes with  $A>87$  resulting from fission of Ta and Ir induced by protons with  $E_p=10.5$  GeV were not measured.

It should be noted that the energy dependence of the dispersion of the Rb isotope distributions for different projectile-target combinations (Fig. 10) shows that at low energies,  $E_p<100$  MeV, when the spread of the fissioning nuclei with respect to  $Z, A$ , and excitation energy has little effect on the broadening of these distributions, the dispersion in the reaction is systematically smaller by a factor of about 1.5–2 than in the  $\text{U}(p,X)\text{Rb}$  reaction.<sup>37,38</sup>

Using the mass spectrometer, we measured the relative independent yields of  $^{76-92}\text{Rb}$  isotopes resulting from fission of Ir (natural mixture of isotopes) induced by protons with  $E_p=1$  GeV (see Fig. 11 and Table VI).

To normalize the measured Rb isotope distribution in absolute magnitude, we interpolated the data available in the literature on the fission of nuclides close to Ir. Using the systematics of the dependence of the fission cross sections on  $Z^2/A$  based on data<sup>29,42</sup> for Ta, W, and Au, we determined the cross section for fission of Ir induced by protons with  $E_p=1$  GeV, which was found to be  $50 \pm 5$  mb. Then, using the mass distributions of the fragments of W



TABLE VI. Cross sections for production of Rb isotopes resulting from fission of Ir (natural) induced by protons with  $E_p=1$  GeV.

$A_{\text{Rb}}$	$\sigma, \mu\text{b}$
76	$0,2 \pm 0,1$
77	$1,5 \pm 0,4$
78	$8 \pm 1$
79	$42 \pm 3$
80	$154 \pm 7$
81	$390 \pm 20$
82	$620 \pm 20$
83	$813 \pm 8$
84	$870 \pm 10$
85	$770 \pm 40$
86	$530 \pm 40$
87	$315 \pm 8$
88	$180 \pm 20$
89	$82 \pm 6$
90	$30 \pm 1$
91	$12 \pm 3$
92	$4 \pm 1$

Note. In these data, we give the errors in only the relative measurements of the yields of Rb isotopes in the mass spectrometer without allowance for the error in the absolute values of  $\sigma$ , which is determined by the error in the  $^{84}\text{Rb}$  production cross section used in the normalization.

and Au fission,<sup>42</sup> we obtained an interpolation estimate of the ratio of the yields of isobar products with  $A=84$  resulting from fission of Ir and Au for  $E_p=1$  GeV, which was found to be  $0.61 \pm 0.06$ . Since the values of  $N/Z$  for Ir (natural) and Au differ by just 0.2%, and the  $^{84}\text{Rb}$  yield is maximal among the products with  $A=84$ , it can be assumed that the ratio of the  $^{84}\text{Rb}$  yields from these nuclei has the same value. Under this assumption, and using the known cross section of the  $^{197}\text{Au}(p,X)^{84}\text{Rb}$  reaction at  $E_p=1$  GeV,<sup>43</sup> we determined the cross section for the production of  $^{84}\text{Rb}$  for a thin iridium target. This was found to be  $0.87 \pm 0.17$  mb and was used to normalize the measured independent relative yields of the other rubidium isotopes.<sup>44</sup>

In the measured Rb isotope distribution for Ir fission induced by protons with  $E_p=1$  GeV (shown in Fig. 11 by the crosses), there is an excess of the yields of the  $^{88-92}\text{Rb}$  isotopes over the Gaussian curve determined by the least-squares method from the  $^{76-86}\text{Rb}$  yields.

The excess is about 4% of the sum of the yields of all the rubidium isotopes. This fact can be interpreted as a manifestation of the new fission mechanism noted in Ref. 25.

To obtain further arguments for such an explanation of the asymmetry of the Rb isotope distribution at  $E_p=1$  GeV, we compared the results of our measurements with

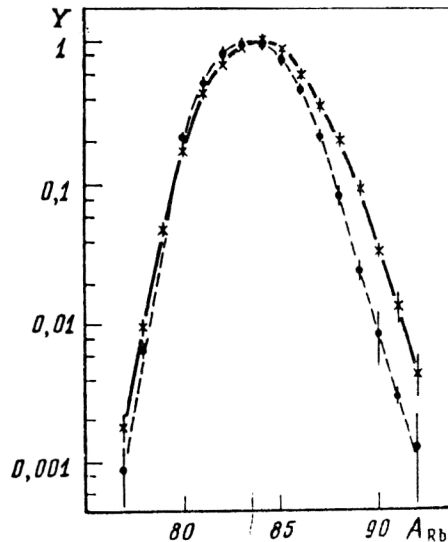


FIG. 12. Relative yields of Rb isotopes in the reactions  $\text{Ta}(^{12}\text{C},X)\text{Rb}$  at  $E(^{12}\text{C})=924$  MeV (Ref. 40, black circles) and  $\text{Ir}(p,X)\text{Rb}$  at  $E_p=1$  GeV (crosses). The data are normalized using the yields of the isotopes  $^{83}\text{Rb}$  and  $^{84}\text{Rb}$  and are connected by curves in order to facilitate comparison of the shapes of these distributions.

data on Ir fission induced by protons with  $E_p \leq 100$  MeV (Ref. 37) and heavy-ion reactions at  $E \leq 77$  MeV per nucleon,<sup>40</sup> in which compound nuclei near iridium are produced. At these energies, the new fission mechanism must, if it is associated with the relativistic energy of the projectile particles, be absent.

In the study of Ref. 40, independent yields were determined for numerous product nuclei, including  $^{77-92}\text{Rb}$ , from fission of  $^{238}\text{U}$  and  $^{181}\text{Ta}$  induced by  $^{12}\text{C}$  ions with  $E=156, 324, 924$  MeV. In the case of the uranium target, a significant difference between the shapes of the Rb isotope distributions for protons with  $E_p=1$  GeV (Ref. 15) and  $^{12}\text{C}$  ions with  $E=924$  MeV (Ref. 40) was not found, whereas the comparison of the  $\text{Ir}(p,X)\text{Rb}$  and  $\text{Ta}(^{12}\text{C},X)\text{Rb}$  reactions for the same energies revealed that the dispersion of the isotope distributions of the products of the second of these reactions was 20% less than for Ir fission (see Fig. 10). Moreover, whereas the yields of the neutron-deficient fragments  $^{77-84}\text{Rb}$  for normalization of these distributions using the maximum (from the  $^{83,84}\text{Rb}$  yields) can be assumed to be the same, within the errors, for both reactions, the yields of the  $^{87-92}\text{Rb}$  isotopes in the reaction with  $^{12}\text{C}$  ions were found to be lower by a factor 2–5 than in the  $\text{Ir}(p,X)\text{Rb}$  reaction (see Fig. 12). Thus, certain features in the mechanisms of the considered nuclear reactions are indeed reflected in the shape of the isotope distributions of the fragments.

Our analysis of the available data on Ta and Ir fission with the production of rubidium isotopes (Refs. 27, 36, 37, and 40) indicates a steady increase in the asymmetry of the isotope distributions of the fragments with increasing energy of the projectile particles in the region  $\sim 1$  GeV and above. The asymmetries of these distributions shown in Fig. 13 were calculated in accordance with the formula

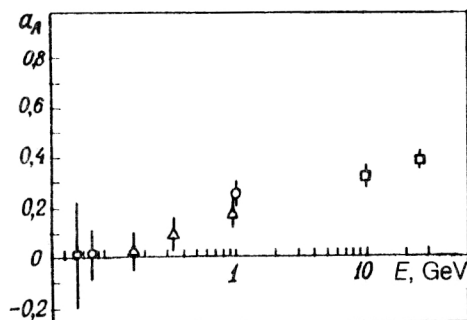


FIG. 13. Asymmetry of Rb isotope distributions as a function of the energy of the projectile particles in the following reactions: Ta( $^{12}\text{C},\text{X}$ )Rb (Ref. 40, open triangles), Ta( $p,\text{X}$ )Rb (Refs. 36 and 40, open squares), and Ir( $p,\text{X}$ )Rb (Refs. 37 and 44, open circles).

$$a_A(\text{Rb}) = \frac{1}{[D_A(\text{Rb})]^{3/2}} \frac{\sum_{A=A_{\min}}^{A_{\max}} (A - A_{\text{av}})^3 Y_A}{\sum_{A=A_{\min}}^{A_{\max}} Y_A}, \quad (13)$$

where  $A_{\text{av}}$  and  $D_A(\text{Rb})$  are the position of the centroid and the dispersion of the Rb isotope distribution;  $Y_A$  is the relative yield of the isotope  $^A\text{Rb}$  with mass number  $A$ ;  $A_{\min}$  and  $A_{\max}$  are the limits of the range of measurements of the Rb isotope distribution. It can be seen from Fig. 13 that in the case of Ir fission induced by protons with energy up to 100 MeV the isotope distributions of the fragments have a

TABLE VII. Cross sections for production of Cs isotopes resulting from interaction of protons with Ir nuclei at  $E_p = 1$  GeV.

$A(\text{Cs})$	$\sigma, \mu\text{b}$
118	$3 \pm 1$
119	$8 \pm 4$
120	$19 \pm 3$
121	$50 \pm 10$
122	$140 \pm 20$
123	$300 \pm 10$
124	$400 \pm 20$
125	$510 \pm 10$
126	$440 \pm 20$
127	$400 \pm 30$
128	$240 \pm 20$
129	$190 \pm 30$
130	$120 \pm 10$
131	$70 \pm 10$
132	$36 \pm 10$
133	$12 \pm 3$

Note. To show the level of the errors in the mass-spectrometric measurements of the relative yields of the cesium isotopes, the error in the absolute normalization of these data, which is the same for all Cs isotopes and is 20%, is not shown in the table.

symmetric form,  $a_A \approx 0$ . However, in the case of Ta and Ir fission induced by protons with  $E_p \gg 1$  GeV, these distributions have a pronounced asymmetry, and this may indicate a difference of the mechanisms of formation of Rb fragments with different values of  $N/Z$ .

Similar investigations were made with the aim of obtaining isotope distributions for  $^{42-48}\text{K}$ ,  $^{80-94}\text{Sr}$ ,  $^{118-133}\text{Cs}$  resulting from interaction of Ir with protons at  $E_p = 1$  GeV. The method of measurements of the relative yields in the case of the potassium and cesium isotopes was similar to that used to investigate the cross sections for  $^{76-92}\text{Rb}$  production.

For the absolute normalization of the results of the Cs measurements we used the estimate obtained above for the Ir fission cross section,  $\sigma = 50 \pm 5$  mb,<sup>42,29</sup> and also the mass distribution of the fragments<sup>42</sup> and the cumulative yields of  $^{127}\text{Xe}$  and  $^{131}\text{Ba}$  from  $^{197}\text{Au}$  (Ref. 43). On the basis of these data, and assuming the same form, we estimated from the isotope distributions of product nuclei with neighboring  $Z$  the cross sections for the production of  $^{127}\text{Cs}$  and  $^{131}\text{Cs}$  in the iridium target at  $E_p = 1$  GeV. From the sum of these values, which was 0.47 mb, and the isotopic Cs distribution obtained using the mass spectrometer, we determined the independent yields of the other cesium isotopes, which are given in Table VII and in Fig. 14.

To obtain the Sr isotope distribution, the method of the measurements with the mass spectrometer "in line" with the accelerator was somewhat modified because the resolution of the instrument was not sufficient to separate the Rb and Sr isobars.

To separate events with production of strontium isotopes, two effects were used: 1) the difference between the

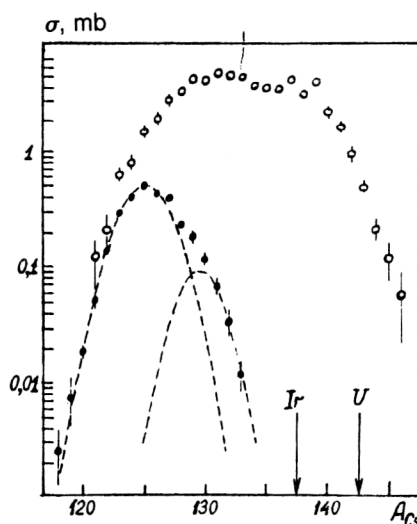


FIG. 14. Cross sections for production of Cs isotopes resulting from interaction of protons with iridium nuclei (black circles) or uranium nuclei (open circles) at  $E_p = 1$  GeV. The data for the uranium target are taken from Ref. 15. The broken curves show the result of decomposing the cesium isotope distribution for the iridium target into two Gaussian curves. The arrows show the values of  $A(\text{Cs})$  corresponding to equality of the  $N/Z$  ratios in the product and target (iridium or uranium) nuclei.

mean time of extraction of the Rb and Sr atoms from the target, which were, respectively, 30 msec and 0.4 sec at  $T_{\text{tar}}=1900^\circ\text{C}$ ; 2) the change in the ratio of the probabilities of surface thermoionization of Sr and Rb from  $\sim 10^{-3}$  for a tantalum ionizer at  $T_i=1700^\circ\text{C}$  to 0.08 for the rhenium ionizer at  $T_i=2000^\circ\text{C}$ .

In the regime of a pulsed proton beam with variation in the detection time delay of the mass spectrometers, we obtained isotope distributions for both Rb and a mixture of Rb and Sr isobars contained in comparable amounts in the mixture. After mutual normalization using the yields of the nuclides with  $A=76-79$ , in which the strontium admixture was negligibly small (less than 4%), from the difference of these distributions we determined the independent relative yields of the Sr isotopes, which are given in Table VIII and in Fig. 15.

As is shown in Fig. 15, the isotope distribution of Sr in the case of Ir fission induced by protons with  $E_p=1$  GeV can be well described by a Gaussian curve, the parameters of which were determined from the  $^{80-86}\text{Sr}$  yields. However, as in the case of the Rb fragments, we observe a systematic excess of the yields of the Sr isotopes above the Gaussian curve in the region of mass numbers next to  $^{95}\text{Sr}$ , whose  $N/Z$  ratio is almost equal to the  $N/Z$  of the target nuclei. If it is borne in mind that for  $E_p < 100$  MeV the

TABLE VIII. Relative independent yields of K and Sr isotopes produced by the interaction of protons with Ir at  $E_p=1$  GeV.

$\text{Ir} + p \rightarrow {}^A\text{K} + X$	
$A(\text{K})$	$Y_A/Y_{42}$
42	1,000
43	$0,90 \pm 0,04$
44	$0,62 \pm 0,04$
45	$0,29 \pm 0,02$
46	$0,13 \pm 0,02$
47	$0,06 \pm 0,02$
48	$0,018 \pm 0,009$
$\text{Ir} + p \rightarrow {}^A\text{Sr} + X$	
$A(\text{Sr})$	$Y_A/Y_{86}$
80	$0,012 \pm 0,007$
81	$0,05 \pm 0,01$
82	$0,18 \pm 0,04$
83	$0,39 \pm 0,08$
84	$0,7 \pm 0,1$
86	1,000
88	$0,7 \pm 0,1$
89	$0,52 \pm 0,06$
90	$0,27 \pm 0,04$
91	$0,17 \pm 0,03$
92	$0,07 \pm 0,02$
93	$0,03 \pm 0,01$
94	$0,010 \pm 0,006$

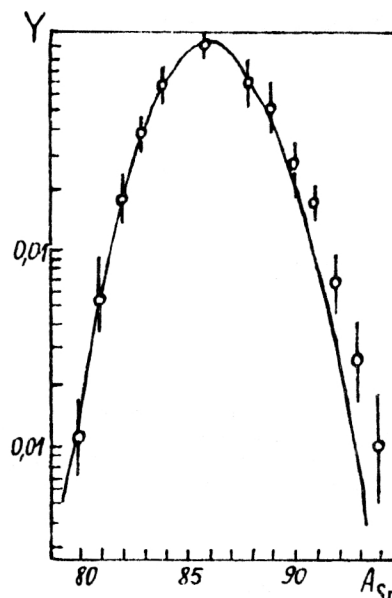


FIG. 15. Relative independent yields of Sr isotopes resulting from the interaction of protons with nuclei at  $E_p=1$  GeV. The continuous curve is a Gaussian distribution with parameters determined from the  $^{80-86}\text{Sr}$  yields.

isotope distributions of the fragments from Ir fission have a symmetric Gaussian form,<sup>37</sup> then the asymmetry of the Sr isotope distribution observed at  $E_p=1$  GeV can be explained by the appearance of a group of neutron-rich fragments having a production mechanism different from that of the bulk of the Sr isotopes. The contribution of this additional group of Sr isotopes is  $5 \pm 2\%$ , in agreement with the Rb data.

It is assumed in Refs. 25, 32, and 45 that pre-equilibrium fission of nuclei occurs as a result of the collective interaction of the projectile particles with the nucleons of the target nuclei in the case of almost central collisions. It is logical to assume that for large collision parameters this process must lead to the production of product nuclei that are traditionally ascribed to deep spallation or fragmentation reactions. Indications of the existence of such events are the features noted in a number of experiments in the angular distributions and in the dispersion of the ranges of the product nuclei with  $A < A_{\text{tar}}/3$  and  $A > 2A_{\text{tar}}/3$  (Refs. 46-48). It would certainly be interesting to find effects associated with this reaction mechanism in the isotope distributions too of such product nuclei.

Both in fission and in spallation reactions, the conjectured process of collective interaction of protons with nuclei will more probably be found among events with very large multiplicity of the accompanying particles.<sup>32,45,48</sup> In this sense, the cesium isotopes are entirely suitable objects for investigation. When they are produced in an iridium target, the total loss of nucleons is  $\Delta A \geq 60$ .

In the case of heavier target nuclei, for example, uranium, it will be extremely difficult to separate the manifestation of the new reaction mechanism expected in the neutron-rich region of the cesium isotope distribution from

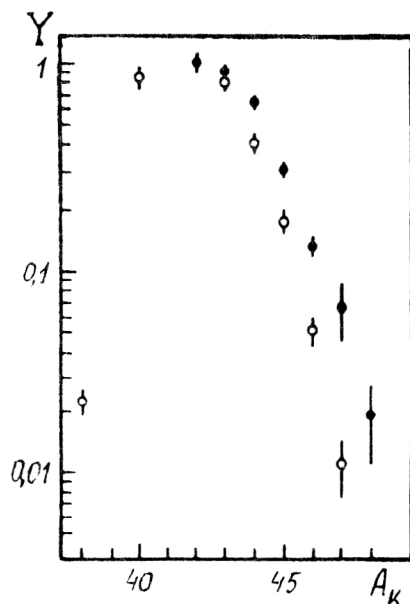


FIG. 16. Relative independent yields of potassium isotopes in two reactions:  $^{181}\text{Ta} + ^{12}\text{C}(924 \text{ MeV}) \rightarrow A_K + X$  (Ref. 40, open circles) and  $^{191,193}\text{Ir} + p(1 \text{ GeV}) \rightarrow A_K + X$  (black circles). The data are normalized to the  $^{42}\text{K}$  yield.

the background of the ordinary fission of weakly excited residual nuclei produced as a result of a weakly branching intranuclear cascade (Fig. 14).

In an iridium target at  $E_p = 1 \text{ GeV}$ , cesium is produced mainly in deep spallation reactions. On the basis of the interpolation estimate of the data on the mass distribution of fragments of binary fission of W and Au nuclei,<sup>42</sup> the contribution of Ir fission events to the yields of Cs isotopes at  $E_p = 1 \text{ GeV}$  is just 15%. As can be seen in Fig. 14, the Cs isotope distribution has a pronounced asymmetry and can be well approximated by two Gaussian curves, the lower of which makes a contribution of 13.5% to the total distribution and is shifted from its maximum by 4.5 a.m.u. in the direction of larger  $A$ .

In Fig. 16, we give the results of measurement of the relative yields of  $^{42-48}\text{K}$  isotopes from an iridium target at  $E_p = 1 \text{ GeV}$ . These can be regarded as products of the fragmentation reaction. Also given are data on the  $^{181}\text{Ta} + ^{12}\text{C}(924 \text{ MeV}) \rightarrow A_K + X$  reaction from Ref. 40, also normalized by the  $^{42}\text{K}$  yield. In these reactions, the composite systems of the target nuclei and the projectile particles have similar  $A$  and  $Z$  values, and this is of interest for comparison.

Unfortunately, these experimental data are not sufficiently complete, and it is difficult to deduce the final shape of the potassium isotope distribution in these reactions. It can only be concluded that in the case of protons with  $E_p = 1 \text{ GeV}$  the distribution in the region of neutron-rich fragments is significantly more extended than in reactions with carbon ions of the same energy. Thus, analysis of the experimental data on Ta and Ir fission indicate a gradual increase in the asymmetry of the isotope distributions in the region of proton energies  $\sim 1 \text{ GeV}$  and above.

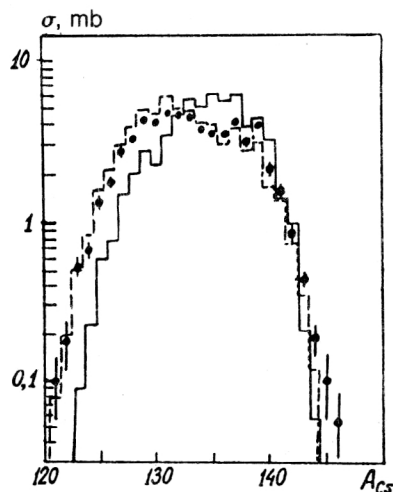


FIG. 17. Results of calculations of yields of Cs isotopes from a  $^{238}\text{U}$  target at  $E_p = 1 \text{ GeV}$  with (continuous line) and without (broken line) allowance for pre-equilibrium emission of particles by the residual nuclei. The points are the experimental data, taken from Table IV.

The asymmetry observed at relativistic proton energies in the experimental isotope distributions of cesium, strontium, and rubidium can be explained by the presence of two mechanisms of proton-nucleus interactions: the cascade-evaporation mechanism, which produces the main group of residual nuclei, and the collective mechanism, which produces a relatively small group of neutron-rich isotopes. In the second case, thermodynamic equilibrium is not established, the residual products have low excitation energy, and the ratio of the number of neutrons to the number of protons in them is close to the ratio in the target nucleus.<sup>49</sup>

## COMPARISON OF CALCULATED AND EXPERIMENTAL DATA

A Monte Carlo calculation was made of the fast stage of the intranuclear cascade for  $10^4$  interactions of protons with  $^{238}\text{U}$  nuclei at  $E_p = 1 \text{ GeV}$ , and the characteristics of the residual nuclei, which are the point of departure for calculating the slow evaporation stage of the reaction, were determined. A calculation was then made of the stage of thermodynamic emission of particles with allowance for the competition by fission, using the form of model described in Refs. 50 and 51.

In the final stage of the calculations, the partial yields of the Rb and Cs isotopes corresponding to the different fissioning nuclei were added together, and this yielded isotope distributions of these elements for  $^{238}\text{U}$  fission induced by protons with  $E_p = 1 \text{ GeV}$ . The calculated Rb and Cs distributions were normalized using the sum of the independent yields of all the Rb and Cs isotopes, the experimental values of which are given in Table IV. Figures 17 and 18 demonstrate the accuracy with which the Cs and Rb isotope distributions were reproduced in the individual versions of the calculations.

It can be seen from Fig. 17 that allowance for the pre-equilibrium emission of particles in the exciton model<sup>52</sup>

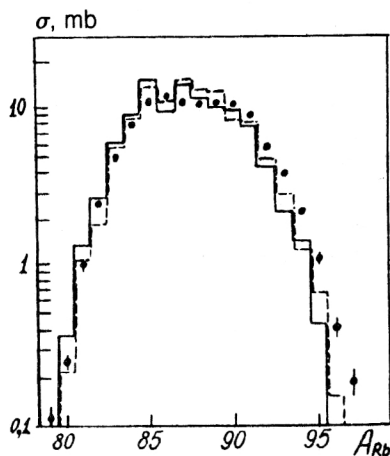


FIG. 18. Results of calculations of yields of Rb isotopes from a  $^{238}\text{U}$  target at  $E_p=1$  GeV without (continuous line) and with (broken line) allowance for the temperature dependence of the fission barriers. The points are the experimental data, taken from Table IV.

leads to a significant suppression of the yields of neutron-deficient fragments, this being due to the sharp lowering of the mean excitation energy of the fissioning nuclei and the reduction in the nucleon and charge losses per fission event (see Table IX). The agreement of this version of the calculation with experiment can be improved if it is assumed that the contribution of the pre-equilibrium stage of particle evaporation is smaller by a factor 1.5–2 than is given by the model used in the calculations. As is shown in Fig. 18, the influence of the temperature dependence of the height of the fission barriers of the residual nuclei in the case of  $^{238}\text{U}$  interaction with protons at  $E_p=1$  GeV is manifested in a small decrease in the ratio of the yields of neutron-deficient and neutron-rich fragments. At the same time, one can achieve the best agreement with the shape of the experimental Rb and Cs isotope distributions if pre-equilibrium emission of particles from the residual nuclei is

completely eliminated. Allowance for the influence of shell effects on the fissility of the nuclei had a very weak effect on the form of the isotope distributions of the fragments, and the corresponding histogram is not given here.

It is interesting to note that in all the calculated versions the yields of fragments with a neutron excess were somewhat too low. This can probably be explained, first, by an insufficiently correct allowance for the contribution of the reaction products from peripheral collisions of protons with target nuclei, which result in the production of residual nuclei with lower excitation energy, and, second, by the contribution of reaction products due to the collective fission mechanism,<sup>46,49</sup> which, as in the case of iridium, must also play a role for the uranium nuclei.

In the calculations, correlations between the characteristics of the fragments of the fissioning and residual nuclei were represented in the form of two-dimensional matrices. Using these data, we determined for each Rb and Cs isotope the mean excitation energies of the fissioning nuclei and the nucleon and charge losses per fission event. The results, averaged over all Rb and Cs isotopes, are given in Table IX for the three versions of calculations used to obtain the Cs and Rb isotope distributions shown in Figs. 17 and 18. The dependence of  $\overline{\Delta A}_{\text{tot}}$  and  $\overline{\Delta Z}_{\text{tot}}$  on the mass number of the isotopes produced as a result of  $^{238}\text{U}$  interaction with protons at  $E_p=1$  GeV has, as is shown in Fig. 19 for the Rb fragments, a linear nature except for the neutron-rich region, which corresponds to low-energy fission.

Thus, in the framework of the cascade–evaporation model it is possible, without any adjustment of model parameters, to reproduce entirely satisfactorily the nature of the change in the shape of the fragment isotope distributions and the multiplicity of light particles with increasing energy of the protons that induce the  $^{238}\text{U}$  fission up to  $E_p=1$  GeV. It may therefore be concluded that the results of the calculations confirm the validity of the assumption used in them that the mechanism of division of the charge

TABLE IX. Calculated mean values of the excitation energy of fissioning nuclei,  $\overline{E}_f$  (in MeV), the nucleon and charge losses before fission,  $\overline{\Delta A}_f$  and  $\overline{\Delta Z}_f$ , and also the total losses per fission event,  $\overline{\Delta A}_{\text{tot}}$  and  $\overline{\Delta Z}_{\text{tot}}$ , in the case of production of Rb and Cs following interaction of  $^{238}\text{U}$  with protons at  $E_p=1$  GeV.

Calculated values		$\overline{E}_f$	$\overline{\Delta A}_f$	$\overline{\Delta Z}_f$	$\overline{\Delta A}_{\text{tot}}$	$\overline{\Delta Z}_{\text{tot}}$
Version of calculation	a	60	13	1,7	19	2,2
	b	170	9	1,4	23	2,6
	c	180	8	1,3	22	2,6
Experiment (Ref. 24) Rb		—	$11,4 \pm 2,1$	—	$22 \pm 4$	—
Experiment (Ref. 15) Cs		—	—	—	$26,4 \pm 0,5$ $18,2 \pm 0,4$	$3,6 \pm 0,3$ $1,3 \pm 0,5$

Note. Results of calculations are given for the following versions: a) with allowance for pre-equilibrium emission of particles by the residual nuclei; b) without allowance for pre-equilibrium emission and the temperature dependence of the height of the fission barriers; c) with allowance for the temperature dependence of the fission barriers. The nucleon and charge losses were determined in accordance with Eqs. (8) and (10) without allowance for the incident protons.



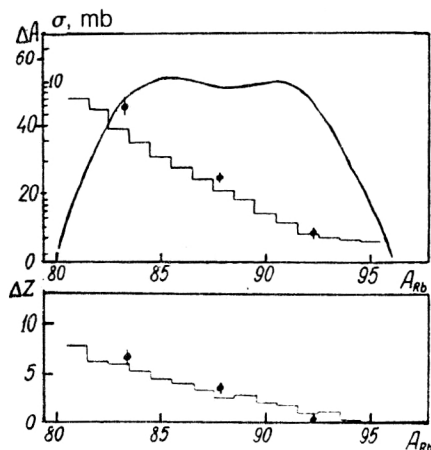


FIG. 19. Dependence of the nucleon and charge losses per fission event on the mass number of the Rb fragments produced as a result of  $^{238}\text{U}$  interaction with protons at  $E_p=1$  GeV (the histograms are the result of the calculation, and the points are the experimental data<sup>15</sup>). The curve shows the Rb isotope distribution.

between the fragments is unchanged for the main group of residual nuclei produced in a given reaction.

The results of the calculations are also in complete agreement with the assumption that the main reason for the broadening of the isotope distributions of the fragments with increasing  $E_p$  in the region of 1 GeV is the growth in the dispersion of the nucleon composition and excitation energy of the residual nuclei.

For an iridium target at proton energy  $E_p=1$  GeV we calculated only the isotope distribution of cesium, the main contribution to which must be made by products of the spallation reaction (about 85%), since the contribution due to fission events is just 15% according to the experimental data. It can be seen from Fig. 14 that the experimental Cs isotope distribution in the  $\text{Ir}+p$  reaction is well approximated by a sum of two Gaussian curves.

To establish whether it is possible to associate the first Gaussian with the production of products in the spallation reaction and the second with fission products, the positions of the centroids for both theoretical Gaussian distributions were determined in the calculations. The calculations were made in the framework of the cascade-evaporation model.<sup>51</sup>

To achieve consistency with the experimental iridium fission cross section, the level-density parameter at the saddle point was increased to  $a_f=0.1035$  for  $a_n=0.1$  (Ref. 44).

TABLE X. Results of calculations, in accordance with the cascade-evaporation model, of the cross sections for production of Cs isotopes in Ir spallation and fission reactions induced by protons with energy  $E_p=1$  GeV.

Calculated values	$\overline{A}(\text{Cs})$	$\sqrt{D_{A(\text{Cs})}}$	$\overline{E_c}(\text{Cs}), \text{ MeV}$	$\overline{\Delta A}_{\text{tot}}$	$\overline{\Delta Z}_{\text{tot}}$
Spallation	126,2	2,22	677	66,0	22,0
Fission	125,9	2,1	458	39,3	9,5
Experiment	$125,78 \pm 0,07$	$2,47 \pm 0,04$	—	—	—

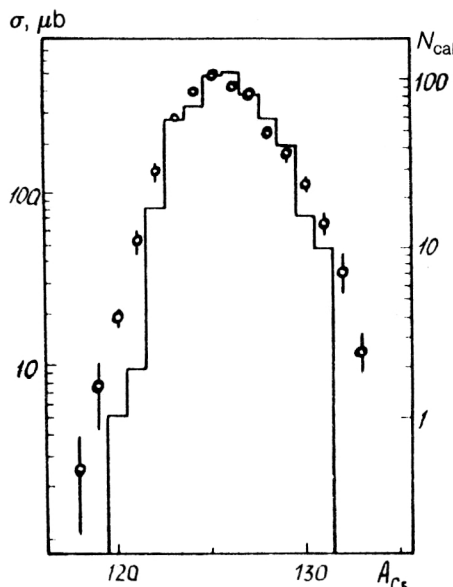


FIG. 20. Comparison of calculated (histogram) and experimental data (points) on Cs yields resulting from interaction of Ir with protons at  $E_p=1$  GeV. Only fission events are taken into account in the results of the calculations made using the cascade-evaporation model.

In the results of the calculations, we determined separately the yield distributions of the cesium isotopes for events with fission of residual nuclei and events for which the excitation energy of the nuclei was reduced solely by the emission of light particles. A calculation was made of more than 23000 inelastic interactions of protons with Ir nuclei at  $E_p=1$  GeV. Table X gives the results of the calculations in accordance with the cascade-evaporation model for the cross sections for the production of Cs isotopes in spallation reactions and Ir fission induced by protons with  $E_p=1$  GeV. For these reactions, we give separately the centroids  $\overline{A}(\text{Cs})$  and the dispersions  $D_{A(\text{Cs})}$  of the cesium isotope distributions, the mean excitation energies of the post-cascade nuclei,  $\overline{E_c}(\text{Cs})$ , and also the mean sums of the masses,  $\overline{\Delta A}_{\text{tot}}$ , and charges,  $\overline{\Delta Z}_{\text{tot}}$ , of all the accompanying particles with  $A \leq 4$  and  $Z \leq 2$ .

As follows from Table X and Fig. 20, the cesium isotope distributions calculated in the framework of the intranuclear-cascade mechanism have, both for spallation of the iridium nuclei and for their fission, parameters very close to the Gaussian distribution describing the experimental yields of the main group of Cs isotopes (the more

neutron-deficient group). It was found that the maxima of the two calculated distributions practically coincide, and, thus, the observed asymmetry of the cesium isotope distribution cannot be explained in the framework of the employed specific version of the model by the superposition of the contributions of the spallation reaction and fission.

In addition, it can be seen from Table X that the calculated excitation energies of the residual nuclei in events with production of cesium isotopes are too high for this asymmetry to be a manifestation of shell effects. It is more probable that the experimentally observed asymmetry of the cesium isotope distribution is, as in the case of the formation of the experimental isotope distributions of the Rb and Sr fragment products typical for Ir, the result of the competition of two different mechanisms of proton-nucleus interaction—the traditional cascade–evaporation mechanism, which makes the main contribution to the experimental yields of Cs isotopes in interaction of Ir with protons at  $E_p=1$  GeV, and some new collective mechanism,<sup>46,49</sup> corresponding to the production of a group of Cs isotopes with higher  $N/Z$  values close to the  $N/Z$  values for Ir. Moreover, the contribution of this new interaction mechanism in the spallation reaction was found to be much more appreciable for Cs (by a factor of about 3) than in events with production of Rb and Sr fragments.

## CONCLUSIONS

1. The isotope dependences of the yields of products of the interaction of protons with different nuclei at  $E_p=1$  GeV have been investigated using an “in line” mass spectrometer. The measurements of the independent relative yields of some isotopes of the product nuclei have been used in a systematic study of even–odd and shell effects in nuclear reactions induced by intermediate-energy protons.

These effects in the nuclear reactions give rise to fluctuations in the yields of the product nuclei with respect to the smooth curves that approximate their isotope distributions. Analysis of the experimental data revealed a systematic excess of the independent yields of isotopes with even numbers of neutrons, especially near closed shells and subshells. The magnitude of the even–odd effect for the yields of the product nuclei in the case of spallation of carbon nuclei reaches  $\sim 50\%$ , while in the case of nuclei of medium mass [in the  $Zr(p,X)Rb$  reaction] it is  $\sim 15\%$ . In the framework of the cascade–evaporation model, the explanation for this is that the influence of the neutron binding energy is stronger than the influence of the difference between the level densities of the residual nuclei.

The even–odd effect was found to become weaker with increasing loss of nucleons in the spallation reaction. This indicates that the influence of the nuclear structure on the yields of the product nuclei becomes weaker with increasing excitation energy of the residual nuclei.

2. It has been shown experimentally that in the case of  $^{238}U$  fission induced by protons with  $E_p=1$  GeV the neutron-rich isotopes of Rb and Cs are the most probable complementary fragments, whereas the neutron-deficient isotopes of these elements are produced in events with very high losses per uranium fission event. We have conjectured

that the two-hump form of the isotope distributions of the fragments can be explained by a high probability of surface reactions in inelastic interactions of protons with uranium nuclei and by the influence of shell effects. Analysis of the isotope distributions of Rb ( $Z=37$ ) and Cs ( $Z=55$ ) suggests that the same mechanism responsible for fission induced by low-energy particles also makes an important contribution at  $E_p=1$  GeV, particularly in the case of the production of neutron-rich fragments.

We have studied the possibility of obtaining phenomenological estimates of the cross sections for production of fragment nuclei for other  $Z$ , and we have also estimated the multiplicity of the neutron and proton losses per uranium fission event.

3. We have investigated the shape of the isotope distributions of K, Rb, Sr, and Cs in fission and spallation of Ir nuclei induced by protons with  $E_p=1$  GeV. The experimentally obtained distributions exhibit an excess in the yields of the neutron-rich isotopes of these product nuclei over the Gaussian curve, the isotopes in excess being  $^{88-92}Rb \approx 4\%$ ,  $^{88-94}Sr \approx 5\%$ ,  $^{128-133}Cs \approx 13.5\%$ . The nucleon composition (the ratio  $N/Z$ ) of these isotopes is close to that of Ir. Analysis of the experimental data on Ta and Ir fission indicates a gradual increase in the asymmetry of the isotope distributions of the product nuclei in the region of  $E_p=1$  GeV and above.

The preferred explanation of the asymmetry of the isotope distributions of Rb, Sr, and Cs at relativistic proton energies is by the presence of two mechanisms of proton-nucleus interaction: the cascade–evaporation mechanism, which gives rise to the main group of residual nuclei, and the pre-equilibrium mechanism, which produces the comparatively small group of neutron-rich product nuclei. In the second mechanism, many nucleons are emitted before thermodynamic equilibrium is established, the residual nuclei have low excitation energy, and the ratio of the number of neutrons to the number of protons in them is close to this ratio for the target nuclei.

4. A new modification of the cascade–evaporation model taking into account the fission process has been used, and it provided the basis for a calculation of some isotope distributions of product nuclei resulting from the interaction of 1-GeV protons with uranium and iridium nuclei. The agreement between the calculated and experimental data was shown to be satisfactory, except in the region of the neutron-rich isotopes.

For the experimental data on iridium, the cascade–evaporation model gives a good description of the production of the bulk of the neutron-deficient products of the fission and spallation reactions. The asymmetry of the isotope distributions cannot be explained by shell effects because the calculated excitation energy of the residual nuclei in events with cesium production is too high.

<sup>1</sup>B. N. Belyaev, L. N. Gall', R. N. Gall' *et al.*, *Prib. Tekh. Eksp.* **4**, 51 (1979).

<sup>2</sup>B. L. Tracy, J. Chaumont, R. Klapisch *et al.*, *Phys. Rev. C* **5**, 222 (1972).

<sup>3</sup>R. Silberberg and D. H. Tsao, *Astrophys. J., Suppl. Ser.* **25**, 315 (1973).

<sup>4</sup>E. S. Izosimova, A. A. Nosov, V. V. Smirnov *et al.*, Preprint RI-87 [in Russian], V. G. Khlopin Radium Institute, Leningrad (1978).

- <sup>5</sup>J. Audouze, M. Epherre, and H. Reeves, Nucl. Phys. **A97**, 144 (1967).
- <sup>6</sup>V. I. Bogatin, E. L. Grigor'ev, O. V. Lozhkin *et al.*, Preprint R1-8715 [in Russian], JINR, Dubna (1975).
- <sup>7</sup>V. V. Avdeichikov, Preprint R4-11262 [in Russian], JINR, Dubna (1978).
- <sup>8</sup>Yu. A. Murin, Preprint RI-117 [in Russian], V. G. Khlopin Radium Institute, Leningrad (1980).
- <sup>9</sup>B. N. Belyaev, V. D. Domkin, Yu. S. Egorov *et al.*, Izv. Akad. Nauk SSSR, Ser. Fiz. **42**, 2392 (1978).
- <sup>10</sup>J. M. D'Auria, L. C. Carraz, P. G. Hansen *et al.*, *Proc. of the Third Int. Conf. on Nuclei Far from Stability (Cargese, France)* (Geneva, 1976), p. 262.
- <sup>11</sup>A. K. Lavrukina, *Nuclear Reactions in Cosmic Rays* [in Russian] (Nauka, Moscow, 1972).
- <sup>12</sup>K. F. Chackett and G. A. Chackett, Nucl. Phys. **A100**, 633 (1967).
- <sup>13</sup>V. S. Barashenkov and V. D. Toneev, *Interactions of High-Energy Particles and Nuclei with Nuclei* [in Russian] (Atomizdat, Moscow, 1972).
- <sup>14</sup>Yu. P. Popov, A. M. Sukhovoï, V. A. Khitrov *et al.*, Preprint R3-84-94 [in Russian], JINR, Dubna (1984).
- <sup>15</sup>B. N. Belyaev, V. D. Domkin, Yu. G. Korobulin *et al.*, Nucl. Phys. **A348**, 479 (1980).
- <sup>16</sup>B. N. Belyaev and V. D. Domkin, Prikl. Yad. Spektrosk. **11**, 145 (1981).
- <sup>17</sup>G. Friedlander, L. Friedman, B. Gordon *et al.*, Phys. Rev. **129**, 1809 (1963).
- <sup>18</sup>M. Epherre, G. Audi, C. Thibault *et al.*, Phys. Rev. C **19**, 1504 (1979).
- <sup>19</sup>S. J. Balestrini and L. Forman, Phys. Rev. C **10**, 1872 (1974).
- <sup>20</sup>J. K. P. Lee, G. Pilar, B. L. Tracy *et al.*, J. Inorg. Nucl. Chem. **37**, 2035 (1975).
- <sup>21</sup>R. Klapisch, *Proc. of the Int. School-Seminar on Reaction of Heavy Ions with Nuclei and Synthesis of New Elements*, D7-19734 (JINR, Dubna, 1976), p. 155.
- <sup>22</sup>M. Rajasekaran and V. Devanathan, Phys. Lett. **104B**, 95 (1981).
- <sup>23</sup>R. Benytsson, P. Moller, and J. R. Nix, Phys. Scr. **29**, 402 (1984).
- <sup>24</sup>M. N. Andronenko, I. N. Sinogeev, G. E. Solyakin *et al.*, Preprint No. 375 [in Russian], Leningrad Institute of Nuclear Physics (1977).
- <sup>25</sup>B. D. Wilkins, S. B. Kaufman, E. P. Steinberg *et al.*, Phys. Rev. Lett. **43**, 1080 (1979).
- <sup>26</sup>N. Sugarman, H. Münzel, J. A. Panontin *et al.*, Phys. Rev. **143**, 952 (1966).
- <sup>27</sup>R. Klapisch, J. Chaumont, J. Jastrzebski *et al.*, Phys. Rev. Lett. **20**, 743 (1968).
- <sup>28</sup>P. C. Stevenson, H. G. Hicks, W. E. Nervik, and D. R. Nethaway, Phys. Rev. **111**, 886 (1958).
- <sup>29</sup>B. A. Bochagov, V. S. Bychenkov, V. D. Dmitriev *et al.*, Yad. Fiz. **28**, 572 (1978) [Sov. J. Nucl. Phys. **28**, 291 (1978)].
- <sup>30</sup>R. L. Hahn and H. W. Bertini, Phys. Rev. C **6**, 660 (1972).
- <sup>31</sup>N. S. Ivanova and I. I. P'yanov, Zh. Eksp. Teor. Fiz. **31**, 416 (1956) [Sov. Phys. JETP **4**, 367 (1957)].
- <sup>32</sup>S. Pandian and N. T. Porile, Phys. Rev. C **23**, 427 (1981).
- <sup>33</sup>B. L. Gorshkov, A. I. Il'in, B. Yu. Sokolovskii *et al.*, Pis'ma Zh. Eksp. Teor. Fiz. **37**, 60 (1983) [JETP Lett. **37**, 72 (1983)].
- <sup>34</sup>D. R. Fortney and N. T. Porile, Phys. Rev. C **22**, 670 (1980).
- <sup>35</sup>B. D. Wilkins, E. P. Steinberg, and S. B. Kaufman, Phys. Rev. C **19**, 856 (1979).
- <sup>36</sup>R. Bernas, Adv. Mass Spectrom. **4**, 919 (1967).
- <sup>37</sup>B. P. Pathak, L. Lessard, L. Nikkinen, and J. K. P. Lee, Phys. Rev. C **25**, 2534 (1982).
- <sup>38</sup>P. A. Beeley, L. Yaffe, M. Chatterjee *et al.*, Phys. Rev. C **28**, 1188 (1983).
- <sup>39</sup>I. Amarel, R. Bernas, J. Chaumont *et al.*, Ark. Fys. **36**, 77 (1967).
- <sup>40</sup>M. De Saint-Simon, S. Haan, G. Audi *et al.*, Phys. Rev. C **26**, 2447 (1982).
- <sup>41</sup>S. J. Balestrini, R. Decker, H. Wollnik *et al.*, Phys. Rev. C **20**, 2244 (1979).
- <sup>42</sup>L. N. Andronenko, L. A. Vaishnene, A. A. Kotov *et al.*, Preprint No. 882 [in Russian], Leningrad Institute of Nuclear Physics (1983).
- <sup>43</sup>S. B. Kaufman and E. P. Steinberg, Phys. Rev. C **22**, 167 (1980).
- <sup>44</sup>B. N. Belyaev, V. D. Domkin, and V. S. Mukhin, Yad. Fiz. **44**, 876 (1986) [Sov. J. Nucl. Phys. **44**, 565 (1986)].
- <sup>45</sup>Yu. A. Chestnov, B. L. Gorshkov, A. I. Iljin *et al.*, Preprint No. 941, Leningrad Institute of Nuclear Physics (1984).
- <sup>46</sup>G. E. Solyakin, Preprint No. 1275 [in Russian], Leningrad Institute of Nuclear Physics (1987).
- <sup>47</sup>K. Aleklett, W. Loveland, T. Lund *et al.*, Phys. Rev. **33**, 885 (1986).
- <sup>48</sup>J. B. Cummings, Phys. Rev. Lett. **44**, 17 (1980).
- <sup>49</sup>B. N. Belyaev, V. D. Domkin, N. P. Filatov *et al.*, *Abstracts of Int. Conf. on 50th Anniversary of Nuclear Fission* (Leningrad, USSR, 16–20 October, 1989) (Leningrad, 1989), p. 70.
- <sup>50</sup>A. S. Iljinov, E. A. Cherepanov, and S. E. Chigrinov, Z. Phys. A **287**, 37 (1978).
- <sup>51</sup>B. N. Belyaev, V. D. Domkin, and S. E. Chigrinov, in *Program of Experimental Investigations Using the Meson Factory at the Institute of Nuclear Research of the USSR Academy of Sciences (Proc. of the Third All-Union Seminar)* [in Russian] (Moscow, 1984), p. 307.
- <sup>52</sup>K. K. Gudima, G. A. Ososkov, and V. D. Toneev, Preprint R4-7821 [in Russian], JINR, Dubna (1974).

Translated by Julian B. Barbour